Technische Universität Kaiserslautern
Fachbereich Elektrotechnik und Informationstechnik
Lehrstuhl für Automatisierungstechnik
Prof. Dr.-Ing. habil. L. Litz

Masterarbeit M 022

Design of an Individual Mobile Measurement of Thermal Comfort

(Entwurf einer mobilen Messung des thermischen Komforts)

Yolla Indria

Betreuer:	**Prof. Dr.-Ing. habil. Lothar Litz**
	Dr.-Ing. Adolfo Bauschspiess
	Dipl.-Ing. Felix Felgner
Beginn:	**24.01.2006**
Ende:	**24.07.2006**

Erklärung

Die vorliegende Arbeit habe ich auf Initiative und unter Anleitung der Betreuer angefertigt. Bei der Erstellung habe ich keine anderen als die angegebenen Hilfsmittel verwendet.

Kaiserslautern, den 24.07.06

……
Yolla Indria

Table of Contents

Table of Contents 1
1 Introduction 4
2 Thermal Comfort Index 5
2.1 Definition of Thermal Comfort 5
2.2 Thermal Comfort Index According to Fanger [Fan72] 6
2.2.1 Predicted Mean Vote (PMV) 6
2.2.2 Heat Balance 7
2.2.3 Predicted Mean Vote 8
2.2.4 Measurement of PMV 10
2.3 Physiological Equivalent Temperature (PET) 11
3 Selection of Sensors 13
3.1 Temperature Sensor 13
3.1.1 Thermocouple 14
3.1.2 Resistive Temperature Device 15
3.1.3 Thermistor 16
3.1.4 Silicon Based Temperature Sensor 16
3.2 Air Velocity Sensor 16
3.3 Physiological Equivalent Temperature (PET) Sensor 17
3.4 Humidity Sensor 18
3.5 Activity Level Sensor 19
3.5.1 Heart Rate Measurement 21
4 Hardware Design 22
4.1 Thermocouple Amplifier 22
4.2 MICAz Platform 23
4.2.1 MICA Expansion Board 24
4.3 Analog to Digital Converter (ADC) 24
4.4 Pulse Receiver 25
4.5 Power Supply 25
4.6 Layout and Circuit Board 26
5 Software Design 29
5.1 Structure of Communication System 29
5.2 TinyOS 29
5.3 Matlab Program 31
6 Localization 34
6.1 Localization Methods 34
6.2 RSSI Measurement 35
7 Measurement Results 40
7.1 Experimental Setup 40
7.2 Measurement at Point P1, Ventilation Mode 41
7.3 Measurement at Point P1, Cooling Mode 42
7.4 Measurement at Point P2, Ventilation Mode 43
7.5 Measurement at Point P2, Cooling Mode 44
7.6 Measurement at Point P3, Ventilation Mode 45
7.7 Measurement at Point P3, Cooling Mode 46
7.8 Measurement at Point P4, Ventilation Mode 47
7.9 Measurement at Point P4, Cooling Mode 48
8 Conclusion and Future Prospects 49

1 Introduction

In the context of the research project of "Ambient Intelligence", a trend-setting application in the area of the building air conditioning is designed. The goal is an individual measurement of the thermal comfort which an individual present in an air-conditioned area feels. Thereby, a comfort index should be used, which is more meaningful than a punctually measured temperature. Such a measure is e.g. the Predicted Mean Vote (PMV) according to ISO 7730, which considers beside the air and the radiant temperature, also the airflow as well as the activity and clothing of a person. Since the airflow is generally dependent on the place, and the activity in general is individually dependent, the comfort index for each person must be determined separately. With this comprehensive monitoring of the perceived comfort, it shall be possible to create an air conditioning that substantially better suits the current need than what is now possible with the usual building measuring technique.

This work covers the following tasks:

- Conception of a thermal comfort measurement as described above which includes the selection of sensors, signal processing and calculation of the comfort indeces PMV and Physiological Equivalent Temperature (PET).
- Development of compact, portable prototypes, in which the sensors are connected to a MICA-node. Over the MICA-node a radio connection shall be installed to a central computer.

In chapter 2, the most important thermal comfort indices will be explained: PMV and PET, heat balance on human body and calculation of PMV. Chapter 3 describes sensors which will be used for the measurement of PMV. Chapter 4 and 5 explain the design of hardware and software, respectively. Chapter 6 describes about a localization concept based on RSSI. The measurement results are presented in chapter 7. The last chapter presents the conclusion of this work and suggestion for extensions for the future.

2 Thermal Comfort Index

2.1 Definition of Thermal Comfort

Thermal comfort based on ASHRAE standard 55-66 is a condition in mind which expresses satisfaction with the thermal environment [Fan72]. In thermal comfort, a person feels that the air temperature, air humidity, air velocity and heat radiation in his surrounding are optimal and he wishes neither warmer or cooler, neither more dry or more wet of air condition [DIN1946].

The reason for creating thermal comfort is first and foremost to satisfy man's desire to feel thermally comfortable [Fan72]. Another reason is to avoid or to react on thermal stresses: cold stress which frequently happens in winter due to low air temperature values and high air velocity values, and heat stress which frequently happens in summer due to high air and radiation temperature values.

The human body doesn't sense thermal parameters such as air temperature, air velocity, air humidity or radiant temperature separately but it registers the effect of all thermal components by thermo receptors and makes a thermoregulatory response to maintain constant internal body temperature.

The description of fluxes involved in heat exchange between the body and the environment (see Figure 1) is written as a heat balance equation (2.1) and is used as a basis model to evaluate thermal comfort.

$$M + W + Q^* + Q_H + Q_L + Q_{SW} + Q_{RE} = 0\,, \tag{2.1}$$

where,

M	metabolic rate
W	mechanical power
Q^*	radiation budget
Q_H	turbulent flux of sensible heat
Q_L	turbulent flux of latent heat (diffusion of water vapor)
Q_{SW}	turbulent flux of latent heat (sweat evaporation)
Q_{RE}	respiratory heat flux (sensible and latent)

All the terms have the unit of power (W). The value will be positive if they result in an energy gain for the body and will be negative if they mean an energy loss of the body.

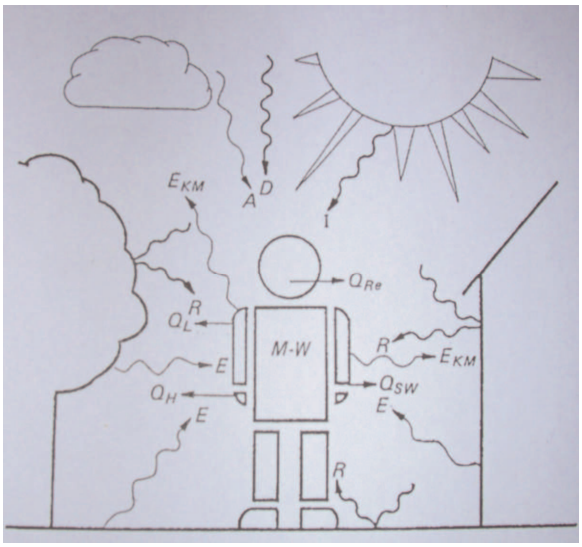

Figure 1: The components in the human heat balance [VDI3787]

2.2 Thermal Comfort Index According to Fanger [Fan72]

2.2.1 Predicted Mean Vote (PMV)

The Predicted Mean Vote (PMV) is a thermal comfort index which was introduced by Fanger in 1970s.

The most important variables which influence the condition of thermal comfort are [Fan72]:

- activity level (heat production in the body),
- thermal resistance of the clothing (clo-value),
- air temperature,
- mean radiant temperature,
- relative air velocity,
- water vapor pressure in ambient temperature.

According to Fanger there are three basic conditions for optimal (desired) thermal comfort ($PMV = 0$). First condition is the existence of heat balance in thermoregulatory system to a given environment. This condition is has general form:

$$f\left(\frac{H}{A_{Du}}, I_{cl}, t_a, t_{mrt}, p_a, v, t_s, \frac{E_{sw}}{A_{Du}}\right) = 0 \qquad (2.2)$$

where,

$\frac{H}{A_{Du}}$ internal heat production per unit body surface are (A_{Du} : DuBois area)

I_{cl} thermal resistance of the clothing

t_a air temperature

t_{mrt} mean radiant temperature

p_a pressure of water vapor in ambient air

v relative air velocity

t_s mean skin temperature

$\frac{E_{sw}}{A_{Du}}$ heat loss per unit body surface area by evaporation of sweat secretion.

For a given activity level, the skin temperature, t_s, and sweat secretion, E_{sw}, are seen to be the only physiological variables influencing the heat balance on equation (2.2). Fanger did some experiments which varies the activity levels. The results are relationships of activity levels to each skin temperature (2.3) and sweat secretion (2.4).

$$t_s = f(\frac{H}{A_{Du}}) \tag{2.3}$$

$$\frac{E_{sw}}{A_{Du}} = A_{Du} f(\frac{H}{A_{Du}}) \tag{2.4}$$

Equations (2.3) and (2.4) are presented as second and third basic conditions of thermal comfort. By substituting the last two conditions to the first one, the comfort equation has the following form:

$$f(\frac{H}{A_{Du}}, I_{cl}, t_a, t_{mrt}, p_a, v) = 0 \tag{2.5}$$

Using comfort equation (2.5), it is possible for any activity level (H/A_{Du}) and any clothing (I_{cl}) to calculate all combinations of remains which will create optimal thermal comfort.

2.2.2 Heat Balance

As mentioned before, the thermoregulatory system of our body maintains a constant internal body temperature, as a reaction to thermal condition of the environment. Therefore, it can be assumed that in reaction to the thermal condition of environment, the heat production of the body will be equal to heat dissipation, and there will be no significant heat storage within the body. The heat balance for this condition is:

$$H/A_{Du} - E_d - E_{sw} - E_{re} - L = K = R + C \tag{2.6}$$

where,

H/A_{Du} the internal heat production in human body

E_d the heat loss by water vapor diffusion through the skin

E_{sw} the heat loss by evaporation of sweat from the surface of the skin

E_{re} the latent respiration heat loss

L the dry respiration heat loss

K the heat transfer from the skin to the outer surfaces of the clothed body

R the heat loss by radiation from the outer surface to the clothed body

C the heat loss by the convection from the outer surface of the clothed body

2.2.3 Predicted Mean Vote

With the thermal comfort equation as a starting point, an index will be derived which makes possible a prediction of thermal sensation for any given combination of thermal parameters.

As a measure for thermal sensation which represents Predicted Mean Vote, a psycho-physical ASHRAE scale is used:

-3	cold
-2	cool
-1	slightly cool
0	neutral
+1	slightly warm
+2	warm
+3	hot

It will be assumed that the thermal sensation at a given activity level is a function of internal heat production, and the heat loss to the actual environment is for a man hypothetically kept at the comfort values of the mean skin temperature and the sweat secretion at the actual activity level.

According to this definition, the thermal load L_t (per unit body surface area) can be expressed mathematically as follows

$$L_t = H/A_{Du} - E_d - E_{sw} - E_{re} - L - R - C \qquad (2.7)$$

In comfort equation, the thermal load will be equal to zero. In other environments the body will change the mean skin temperature and sweat secretion to maintain the internal temperature of the body. Therefore we can conclude the relationship between thermal sensation (which is expressed by the mean vote Y), and the thermal load which might vary with the internal heat production H/A_{Du}. This relationship can be mathematically expressed as follows:

$$Y = f\left(L_t, \frac{H}{A_{Du}}\right) \qquad (2.8)$$

Fanger conducted experiments by varying thermal load and voting thermal sensation. The result shows that $\frac{\delta Y}{\delta L_t}$ has an exponential proportion to the metabolic rate as follows:

$$\frac{\delta Y}{\delta L_t} = 0.303e^{-0.042(M/A_{Du})} + 0.028 \quad (2.9)$$

By integration we then arrive at:

$$Y = (0.303e^{-0.042(M/A_{Du})} + 0.028)L \quad (2.10)$$

The expression for Y given in the last equation will be referred to as the "Predicted Mean Vote" (PMV). By inserting this equation to expression for L in equation (9), the formula for PMV is obtained:

$$PMV = (0.303e^{-0.042(M/A_{Du})} + 0.028)\left(H/A_{Du} - \mathrm{E_d} - \mathrm{E_{sw}} - \mathrm{E_{re}} - \mathrm{L} - \mathrm{R} - \mathrm{C}\right) \quad (2.11)$$

The individual terms are calculated as follows, with unit area W/m^2:

- Internal heat production per unit area

  $$H/A_{Du} = M/A_{Du}.(1-\eta) \quad (2.11a)$$

  The internal heat H is the sum of the metabolic rate M and the mechanical power W ($H = M + W$, mechanical efficiency $\eta = W/M$).

- Water vapor diffusion through the skin

  $$E_d = 0.305 \cdot (57.3 - 0.07.H/A_{Du} - e) \quad (2.11b)$$

- Heat loss by evaporation of sweat

  $$E_{sw} = 0.42 \cdot (H/A_{Du} - 58) \quad (2.11c)$$

- Latent heat loss through respiration

  $$E_{re} = 0.0017 \cdot M/A_{Du} \cdot (58.7 - e) \quad (2.11d)$$

- Sensible heat loss through respiration

  $$L = 0.0014 \cdot M/A_{Du} \cdot (34 - t_l) \quad (2.11e)$$

- Radiative heat flux

$$R = 3.95 \cdot 10^{-8} \cdot f_{cl} \cdot \left[(t_{cl} + 273)^4 - (t_{mrt} + 273)^4 \right], \quad (2.11f)$$

f_{cl} being the surface enlargement factor for the clothed body

$$f_{cl} = 1.0 + I_{cl} \cdot 0.15 \quad (2.11g)$$

- Convective heat flux

$$C = f_{cl} \cdot h_c \cdot (t_{cl} - h_l), \quad (2.11h)$$

where h_c is the heat transfer coefficient and determined by:

$$h_c = \begin{cases} 2.05 \cdot (t_{cl} - t_l) & \textit{for free convection} \\ 12.1 \cdot \sqrt{v_r} & \textit{for forced convection} \end{cases}, \quad (2.11i)$$

and t_{cl} is the surface temperature of the clothing and determined by the equation:

$$t_{cl} = t_s - 0.155 \cdot I_{cl} \cdot (R - C), \quad (2.11j)$$

where the mean skin temperature t_s is obtained by the following empiric numerical equation:

$$t_s = 35.7 - 0.0275 \cdot H / A_{Du} \quad (2.11k)$$

Equation (2.11k) can be solved by the Newton approximation.

2.2.4 Measurement of PMV

PMV can be determined from one of the following ways [ISO7730]:

- using equation (2.11),
- using PMV-tables for several combinations of activity level, operative room temperature, and relative air velocity,
- by direct measurement with application of an integrated temperature sensors.

The operative room temperature t_{OP} is a uniform temperature where an object would have the same amount of heat quantity by radiation and convection. In practice, under the conditions of low air velocity (< 0.2 m/s) or small differences between mean radiant temperature and air temperature (< 4°C), the average of air and mean radiant temperature can be simply be used as operative room temperature.

For more accuracy of operative room temperature the following form should be used [ISO7730]:

$$t_{OP} = At_a + (1 - A) \cdot t_r \tag{2.12}$$

The value of A is a function of relative air velocity v_r as written in the following Table 1:

v_r	<0.2	0.2 – 0.6	0.6 – 1.0
A	0.5	0.6	0.7

Table 1: Constants for operative temperature function

2.3 Physiological Equivalent Temperature (PET)

The evaluation parameter PET (Physiological Equivalent Temperature) was developed from the MEMI (Munich Energy Balance Model for Individuals) energy balance model for the human body [Höp84].

PET is defined as physiological equivalent temperature at any given place (outdoors and indoors) which is equivalent to the air temperature at the reference environment.

The reference environment has a typical indoor setting as follows: radiant temperature is equal to air temperature, air velocity 0.1 m/s, water vapor is 12hPa or approximately equal to a relative humidity of 50% at air temperature 20°C [Höp99]. The assessment is made for a standard "Michel model": 35 years old, 1.80m tall, 75 kg weight man. He performs light activity of 80W and wears clothing with resistance 0.9 clo.

The procedures of calculating PET consists of two steps. The first step is calculating the thermal conditions of human body (physiological variables) under his environment parameters. Unlike PMV calculation, in which the mean skin temperature and the sweat rate are being only dependent on activity and not climatic, MEMI incorporates the real values for skin temperature and the evaporation of sweat. These two unknown variables are calculated by solving the heat fluxes equation from the core of the body to the surface of skin and from the skin to the surface of clothing. As a result, MEMI provides the following physiological variables:

- Core temperature of the body
- Mean skin temperature
- Rate of sweating
- Wetting of the skin
- Individual heat fluxes

These calculated values are then inserted to the MEMI model to solve the air temperature (under reference conditions) which will produce the equal mean skin and body core temperatures. This air temperature is the PET. Some calculated PET values for different climate scenarios are given in the following Table 2.

Scenario	T_a (°C)	T_{mrt}(°C)	v(m/s)	VP (hPa)	PET (°C)
Typical room	21	21	0.1	12	21
Winter, sunny	-5	40	0.5	2	10
Winter, shade	-5	-5	5.0	2	-13
Summer, sunny	30	60	1.0	21	43
Summer, shade	30	30	1.0	21	29

Table 2: PET values for different climate scenarios [Höp99]

As PET is independent of the activity and the clothing, PET cannot be an absolute measure of the thermal comfort or thermal strain because, for example, somebody would feel very cold at PET 20°C if wearing only swimming trunks while he would sweat when wearing a coat. If he were working hard, he would assess this PET value as "too warm" while such thermal condition at rest might be regarded as "too cool".

PET therefore can only be regarded as a basis for an assessment of the thermal environment that has to be adjusted to the subjective characteristics in terms of clothing and activity. It is also difficult to use PET as a set point of air conditioning controller, as there is no fixed PET value which represents a comfort condition of each person.

The thermal perceptions which represent the value of PET are listed in Table 3 below.

PET (°C)	Thermal Perception
4	Very cold
8	Cold
13	Cool
18	Slightly cool
23	Comfortable
29	Slightly warm
25	Warm
41	Hot

	Very hot

Table 3: Ranges of PET for different grades of thermal perception by human beings [Mat99]

3 Selection of Sensors

3.1 Temperature Sensor

Most popular temperature sensors used today are:

- Thermocouple
- Resistive temperature device (RTD)
- Thermistor
- Integrated silicon based sensor

Each of these sensors orientates to specific temperature ranges and environmental conditions. Characteristics of the each sensor decide whether it is suitable for certain application. Some sensors, their characteristics and applications are described in Table 4 and 5 [Bak98]:

Characteristics	Thermocouple	RTD	Thermistor	Integrated Silicon
Temperature Range	270 to 1800°C	250 to 900 °C	100 to 450°C	-55 to 150°C
Sensitivity	10s of μV /°C	0.00385Ω/Ω/ °C (Platinum)	Several Ω/Ω/ °C	Based on technology: 2mV/°C
Accuracy	±0.5°C	±0.01°C	±0.1° C	±1°C
Linearity	Requires at least a 4^{th} order polynomial or equivalent look up table.	Requires at least a 2^{nd} order polynomial or equivalent look up table.	Requires at least 3^{rd} order polynomial or equivalent look up table.	At best within ±1°C. Linearization required.
Ruggedness	The larger gage wires of the TC make it more rugged.	RTDs are susceptible to damage as a result of vibration.	Generally thermistors are more difficult to handle, but not affected by shock or vibration.	As rugged as any IC housed in a plastic package such as dual-in- or surface outline ICs.
Responsive-ness in stirred	< 1 Sec	1 to 10 Secs	1 to 5 Secs	4 to 60 Secs

oil				
Excitation	None	Current Source	Voltage Source	Voltage Sup.
Form of Output	Voltage	Resistance	Resistance	Voltage, Current, or Digital
Typical Size	Bead diameter = 5 x wire diameter	0.25 x 0.25 in.	0.1 x 0.1 in.	From TO-18 Transistors to Plastic DIP
Price	$1 to $50	$25 to $1000	$2 to $10	$1 to $10

Table 4: Temperature sensors characteristics

Sensor Type	**Application**
Thermocouple	Extremely high temperature sensing, biophysics, metal cutting research, gas chromatography, internal combustion engine temperatures, chemical reactions
RTD	Cold junction compensation, bridge temperature, calibration, process control.
Thermistor	Cold junction compensation, bridge temperature sensing, pyrometer calibration, vacuum manometers, anemometers, flow meters, liquid level, fluid velocity, thermal conductivity cells, gas chromatography
Silicon Based	Cold junction compensation, personal computers, office electronics, cellular phones, HVAC, battery management, four speed controls

Table 5: Temperature sensors and their applications

3.1.1 Thermocouple

The thermocouple consists of two dissimilar metals that are soldered together at one end (junction) as shown in Figure 3. This end is put at temperature to be measured and called measuring junction, while another end is at reference temperature and called reference junction. Temperature difference between both junctions will cause an electrical potential difference (voltage). This effect is known as Seebeck effect. Voltage generated is dependent on type of thermocouple (materials of metal) and the temperatures difference. For example, the type K thermocouple has a Chromel positive leg and Alumel (nickel / 5% aluminum and silicon) negative leg, and has Seebeck effect of 40 μV /°C.

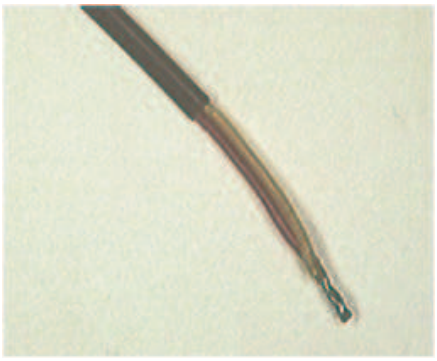

Figure 3: Measuring junction of a thermocouple

A polynomial equation is used to convert thermocouple voltage to temperature (°C) over a wide range of temperatures. We can write the polynomial as:

$$T = \sum_{n=0}^{N} a_n \cdot v^n \qquad (3.1)$$

The coefficients are dependent on type of thermocouple. For example, the coefficients for type K thermocouple are listed in the following Table 6:

n	a_n
0	0.226584602
1	24152.10900
2	67233.4248
3	2210340.682
4	-860963914.9
5	4.83506×10^{10}
6	-1.18452×10^{12}
7	1.38690×10^{13}
8	-6.33708×10^{13}

Table 6: Coefficients for type K thermocouple

3.1.2 Resistive Temperature Device

The RTD (Resistance Temperature Detector) is a resistive element constructed from metals, such as, Platinum, Nickel or Copper. The particular metals that are chosen exhibit a predictable change in resistance with temperature.

The linear relationship between resistance and temperature of the RTD simplifies the implementation of signal conditioning circuitry. The resistance change to temperature varies for each of these types of RTDs.

Platinum RTD (PRTD) is the most accurate and reliable compared to Nickel and Copper. Therefore, it is best suited for precision applications where absolute accuracy and repeatability is critical. The platinum material is less susceptible to environmental contamination, where copper is prone to corrosion causing long term stability

problems. Nickel RTDs tolerate environmental conditions fairly well, however, are limited to smaller temperature ranges.

3.1.3 Thermistor

If accuracy is a high priority, the thermistor should be the temperature sensor of choice. Thermistors are available in two variants, NTC and PTC. The NTC (negative temperature coefficient) thermistor is constructed of ceramics composed of oxides of transition metals (manganese, cobalt, copper, and nickel). With a current excitation the NTC has a negative temperature coefficient that is very repeatable and fairly linear. These temperature dependent semiconductor resistors operate over a range for -100°C to 450°C. Combined with the proper packaging, they have a continuous change of resistance over temperature. This resistive change versus temperature is larger than which are from RTD, consequently the thermistor is systematically more sensitive.

3.1.4 Silicon Based Temperature Sensor

The integrated circuit temperature sensors offer another alternative for solving temperature measurement problems. The advantages of integrated circuit silicon temperature sensors are user friendly output formats and ease of installation in the PCB assembly environment. Since the silicon temperature sensor is an integrated circuit, integrated circuit designs can be easily implement on the same silicon as the sensor. This advantage allows the placement of the most challenging portions of the sensor signal conditioning path to be included in the IC chip. Consequently, the output signals from the sensor, such as large signal voltages, current, or digital words, are easily interfaced with other elements of the circuit. On the other hand, it has relative low accuracy and temperature range of this sensor compared with other sensors.

3.2 Air Velocity Sensor

Since in thermal comfort measurement the temperature will mainly be measured, the technique of air velocity measurement which utilizes temperature measure is preferred. This method is called thermal anemometry.

Thermal anemometer measures the velocity at a point in flowing fluid, either liquid or gas. It consists of two sensors, a velocity sensor and a temperature sensor. The temperature sensor measures the temperature. The electronic circuit passes current to velocity sensor, thereby heating it to a constant temperature differential (T_v-T_a) above the gas temperature and measures the heat qc carried away by the airflow as it flows past the sensor. Hence, it is called “constant temperature thermal anemometer”. Illustration of this method can be seen on Figure 4 below.

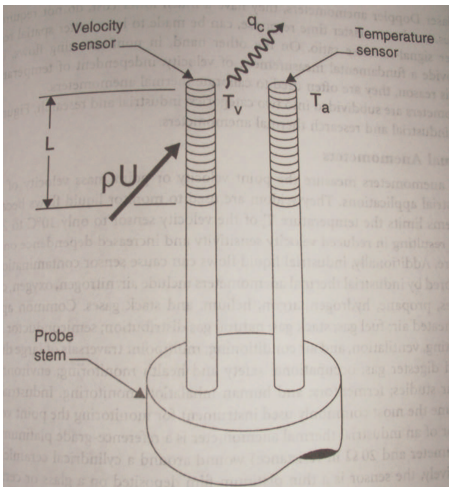

Figure 4: Principle of operation of typical thermal anemometer [Spr99]

Another type of thermal anemometer is constant current thermal anemometer. This method utilizes the same physical principle but in the different way. The electronic circuit provides the velocity sensor with a constant heat, with aim to warm it at a constant temperature. As the fluid flows the temperature will decrease. The temperature decrease is measured and become a measure of flow velocity.

3.3 Physiological Equivalent Temperature (PET) Sensor

The Physiological Equivalent Temperature (in German: Gefühlte Temperatur) sensor from the manufacturer Vereta GmbH offers simultaneous measurement of operative room temperature and air velocity. The sensor consists of a pair thermocouple of type K. The first thermocouple is called passive sensor and measures operative room temperature T_{OP}. The second thermocouple is called active sensor, where its measuring junction is heated by connecting it a constant voltage supply 5 volt. This heater will simulate thermoregulatory of human body which tries to maintain temperature of measuring junction at 34°C. As the air flows past the sensor, the temperature at measuring junction will decrease then using this temperature difference the velocity can be calculated.

This method is contrary to constant temperature thermal anemometer, which supplies more current if the air flows past the sensor. The advantage is no need of electrical circuit that controls heat supply to maintain constant temperature. Because thermocouple only measures temperature difference between its junctions, another sensor must be installed to provide reference temperature. For this aim, a silicon-based temperature sensor TMP01 is selected because this IC is already available at our laboratory and has 1°C accuracy. TMP01 outputs a voltage proportional to the temperature using a scale factor $5mV/K$, which results 1.49V for 25°C.

The PET, air velocity v, and operative room temperature T_{OP} are calculated using the formulas from the manufacturer Vereta GmbH as written below:

$$PET = ((\Delta T_{active} - T_{reference} - 13.00) \cdot 1.05) + T_{reference} \quad (3.2)$$

$$v = (\Delta T_{passive} - \Delta T_{active} + 14.4) \cdot 0.06 \quad (3.3)$$

$$T_{OP} = \Delta T_{passive} + T_{reference} \quad (3.4)$$

The equation (3.3) is valid for maximum air velocity 0.4 m/s. The relationship between temperature difference from active and passive sensor and the air velocity is shown in the Figure 5.

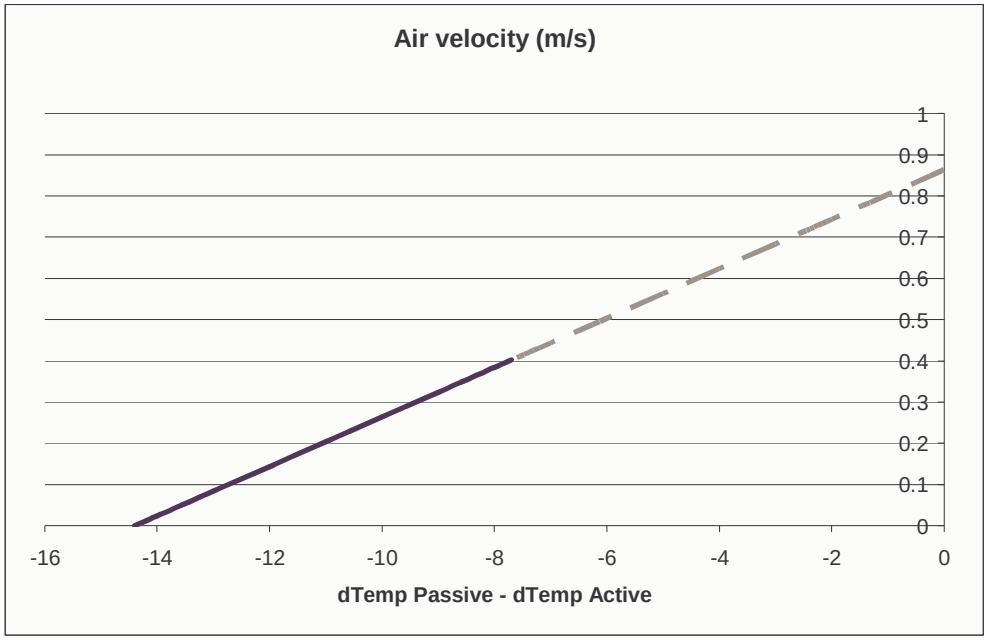

Figure 5: Air velocity

3.4 Humidity Sensor

Humidity is the amount of water vapor in air or other gas. There are two basic method units of humidity measurement, absolute and relative humidity. Absolute humidity is mass of water vapor in a given volume. The unit of absolute humidity is kg/m^3. Relative humidity is ratio of water vapor pressure to water vapor pressure required for saturation, the unit for relative humidity is %RH.

Methods of measuring humidity:

- Hygrometric

  In this method, the sensor is coated with a suitable material that absorbs moisture / water vapor in air. It weighted before and after to determine how much water vapor took out from air.

  Another type of hygrometer works on the principle that electrical resistance or capacity varies in a material that absorbs moisture, with the resistance to a current passing between wires measured by special sensors.

- Psychrometric

Relative humidity is determined using phychrometric chart and temperature reading of two thermometers. First, which is called the dry-bulb thermometer, reads air temperature, while the other one, the wet-bulb thermometer reads the temperature of adiabatic saturation.

- Renode moisture sensing methods

  This method measures the absorption of either microwaves or infrared. Moistured air is irradiated with light in the near infrared spectrum. The reflectance or absorbance of moisture by the rays changes markedly at specific wavelengths proportionally to the moisture content of the air.

Normally, the humidity varies only slightly from one point to other points in a closed room. Therefore, one sensor in each room is enough to measure the humidity. Moreover, the sensitivity of PMV to humidity is rather low comparing to other factors. For this system, an installed humidity sensor from Landis & Steafa is used. The humidity value is available to read from a Simulink block in Matlab.

3.5 Activity Level Sensor

To measure an activity level means to measure the energy expenditure during an activity. The measurement of energy expenditure of a man depends on the following principle [UNU84]:

“All the energy used by the body in carrying out either external or internal work (such as the movements of the heart and respiratory muscles, etc.), or in chemical synthesis such as manufacture of enzymes or hormones, or in maintaining the ionic gradients between the fluids inside and outside the tissue cells, is ultimately degraded into heat. A measurement of heat output of the body is thus also a measure of its energy expenditure. This measurement may be done under laboratory conditions in a specially designed box and is called direct calorimetry.”

Because energy available in food can be liberated in the body and used for above processes only as a result of oxidations, a measurement of the oxygen uptake by the body is also a measure of energy expenditure. This measurement is called “indirect calorimetry”.

To perform such as indirect calorimetry, an instrument such as Max-Planck respirometer is needed. This instrument is principally a gas meter and measures oxygen uptake by a person’s body during a specific activity. The formula needed to calculate energy expenditure is as follows: Energy(kcal/min) = Vstp x Oi-Oe/20, where Vstp is the volume of air expired in liters per minutes, and Oi and Oe are the percentages of oxygen in inspired and expired air, respectively. For this measurement, valves, mount-pieces and mask are also applied to the person. Because of its complicatedness, this measurement method can’t be applied to daily use.

Another indirect assessment of energy expenditure may also be attempted by heart rate recording. In any individual, there is a relationship between heart rate and oxygen consumption, and this relationship is the basis for monitoring the physical activity by recording heart rate.

A study from Hiiloskorpi, 1999 [Hii99] evaluated the ability to use the relationship between heart rate and oxygen uptake to estimate energy expenditure during physical activity. Some groups of men and women carried out two tests one with cycle ergometer and another on a treadmill. Respiratory gases then obtained from indirect calorimetry. Energy expenditure during this activity (AEE) was calculated from oxygen uptake and carbon dioxide production. Using the generalized liner model, two alternative models were found to predict AEE and HR. Both models showed three-way interaction between HR, body weight, and gender.

Further research also by Hiiloskorpi, 2003 [Hii03] evaluated the ability to use the relationship between heart rate and oxygen uptake to estimate energy expenditure from low to high physical activity levels with different HR-based prediction equations.

There are three types of prediction model based on which HR variable it is used. First model uses HR, second model uses HRR and third model uses HRnet.

HRR is the percentage of HR reserve and calculated as follows:

$$HRR = 100 \cdot [(activity\ HR - resting\ HR)/(\max imal\ HR - resting\ HR)] \qquad (3.5)$$

HRnet is the difference between activity HR and resting HR and calculated as follows:

$$HRnet = (activity\ HR - resting\ HR) \qquad (3.6)$$

For this work, only the first model is used in order to avoid additional measurement of resting HR.

Predicted energy expenditure (EE) equations for the first model are presented separately for women and men at different activity levels as follows [10]:

For women with low activity level:

$$EE = -4.70 + 0.0449 \cdot HR - 0.0019 \cdot weight + 0.00052 \cdot HR \cdot weight \qquad (3.7)$$

Here, low activity level refers to activity which needs less than 3 MET.

For women with high activity level:

$$EE = -5.92 + 0.0577 \cdot HR - 0.0167 \cdot weight + 0.00052 \cdot HR \cdot weight \qquad (3.8)$$

For men with low activity level:

$$EE = 4.56 - 0.0265 \cdot HR - 0.1506 \cdot weight + 0.00189 \cdot HR \cdot weight \quad (3.9)$$

For men with high activity level:

$$EE = 3.56 - 0.0138 \cdot HR - 0.1358 \cdot weight + 0.00189 \cdot HR \cdot weight \quad (3.10)$$

The unit for HR is beats per minute (bpm) and unit for EE is kcal/min.

3.5.1 Heart Rate Measurement

The heart rate can easily be taken at any spot on the body at which an artery is close to the surface and a pulse can be felt. The most common places to measure heart rate using the palpation method are at wrist and the neck. This measurement method is often found in integrated blood pressure monitors and pulse monitor. The sensor element is a piezo-film which is very sensitive to mechanical movement. Because the film detects physical motion on skin surface, the measurement must be done when the arm is motionless. Therefore this sensor is suitable short measurement and not for all day use.

Another device, which is more suitable to measure heart rate of a person during daily activity, is heart rate monitor. This device is common among professional athletes and amateurs to monitor their fitness and training intensity. It consists of two parts: a transmitter attached to a belt worn around the chest, and a receiver worn on the wrist like a watch (see Figure 6).

Figure 6: Heart rate monitor

As the heart beats, an electrical signal is transmitted through the heart muscle in order for it to contract. This electrical activity can be detected through the skin as an electrocardiogram signal (ECG). The transmitter part of the heart rate monitor is placed on the skin around the area that the heart is beating, and picks up this signal. The transmitter then sends an electromagnetic signal containing heart rate data to the wrist receiver which displays the heart rate.

4 Hardware Design

4.1 Thermocouple Amplifier

Thermocouple type K delivers voltage about 40 μV/°C which means temperature difference between measuring and reference junction 1°C thermocouple will produce only 0.04mV. Meanwhile the ADC which will be used is 10 bits with input range from 0-3V. ADC voltage resolution is 2.9mV. Without an amplifier, one step quantization of ADC means the temperature change of 72.5°C. Therefore, a signal amplifier is very important for the accuracy of temperature reading.

The selected amplifier is a low cost, precision instrumentational amplifier INA114. Its versatile 3-op amp design and small size make this amplifier ideal for a wide range of applications (see Figure 7). It needs only a single external resistor to set gain from 1 to 10.000, operates on low quiescent current as 3mA, and needs minimum voltage supply as ±2.25V.

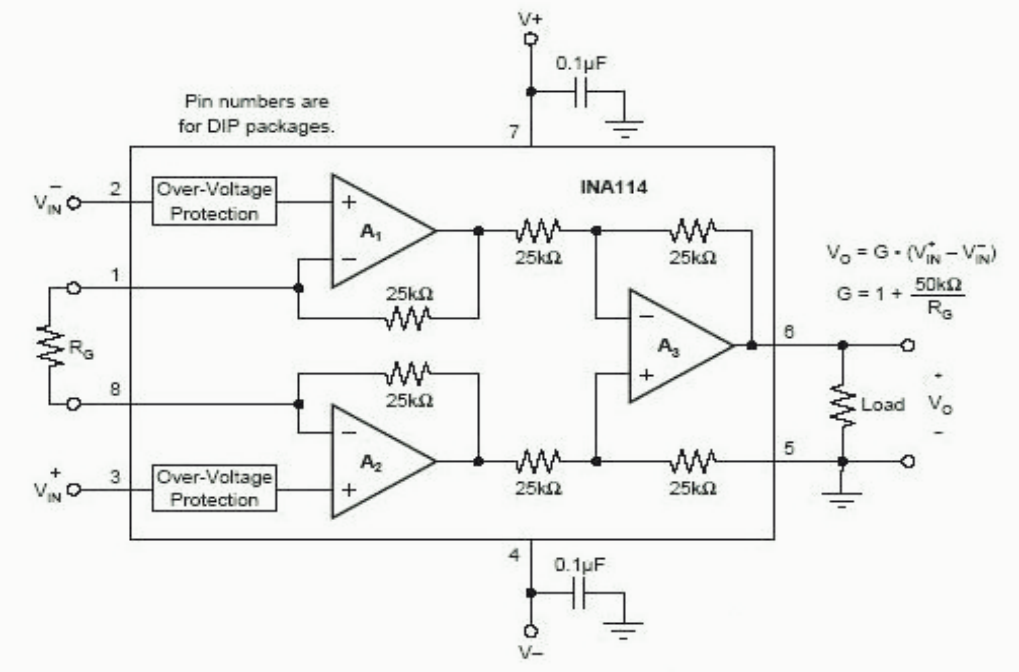

Figure 7: Pin connections and 3op-amp design inside INA114

Bipolar voltage supply makes possible to amplify negative voltage signal from thermocouple which might be happen to passive sensor when measuring junction is colder than reference junction. But because the ADC has only unipolar mode, the negative output from amplifier must be compensated by applying a positive voltage

on reference pin (pin 5) of INA114 instead of ground. In this case, the equation used to calculate Vo is changed to:

$$V_o = G \cdot (V_{IN}^{+} - V_{IN}^{-}) + V_{ref} \quad (23)$$

Furthermore, positive voltage on reference pin would not disturb the operation of the op-amp but only reduce the amplifier's range. In figure 8 and 9 below are simulation result of amplification which designed for passive and active sensor, respectively.

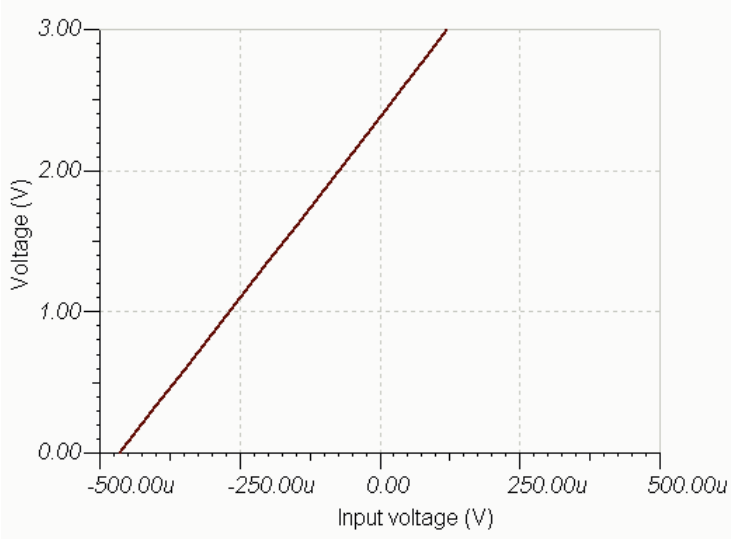

Figure 8: Amplification curve for passive sensor with gain of 5001 and V_{ref} of 2.5 V

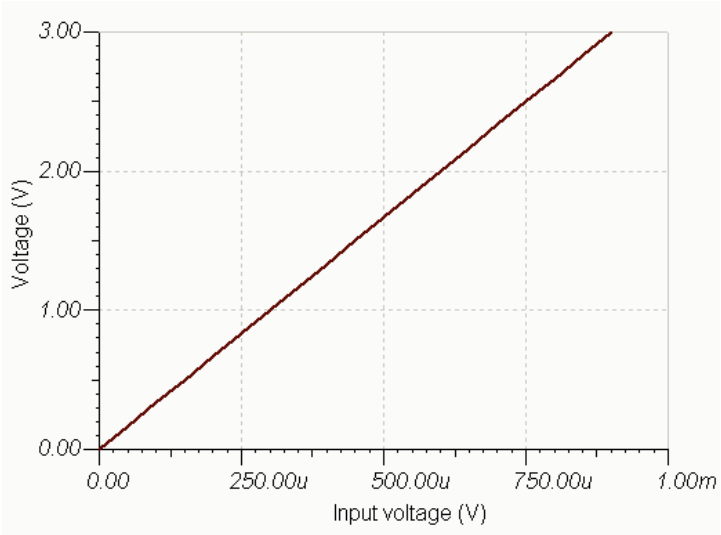

Figure 9: Amplification curve for active sensor with gain of 3334

4.2 MICAz Platform

The MICAz is the latest generation of Nodes from Crossbow Technology used for enabling low power wireless sensor networks (see Figure 10). The MPR2400 / MICAz is build up by components as follows:

- Chipcon CC2420, a radio frequency transceiver with 2.4 GHz frequency
- ATmega128L micro-controller.
- Battery holder for 2xAA batteries
- A Hirose connector, which enables connection to other modules

Figure 10: Photo of the MPR2400-MICAz

4.2.1 MICA Expansion Board

MICA expansion board is a modification of the MIB510 interface board (see Figure 11). It is a multi-purpose interface board used with the MICAz, and some other older platform e.g. MICA2. The board supplies power to the device through an external power adapter, and provides an interface for RS-232 Node serial port and parallel programming port.

The RS-232 interface is a standard single channel bi-directional interface with a DB9 connector to interface to an external computer. It uses transmit and receive lines only.

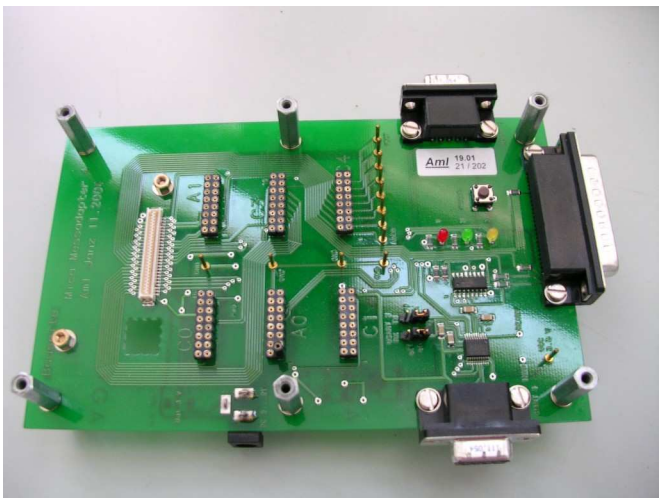

Figure 11: MICA expansion board

4.3 Analog to Digital Converter (ADC)

An embedded ADC from MICAz will simply be used to convert voltages from sensors to digital values. The ADC has 8 channels with 10 bits resolutions which refer to voltage from 0V to supply voltage of MICAz. For power supply for the board, rechargeable batteries are used. The voltage of these batteries may vary due to time of consuming. This voltage will also be taken because it indicates the maximum count of ADC. The ADC channel assignment is given in the Table 7 below:

ADC channel	Assignment
0	Compensator voltage for passive sensor
1	Amplified voltage of passive sensor
2	Amplified voltage of active sensor
3	Output (voltage) of reference temperature sensor.
30	Supply voltage of MICAz

Table 7: ADC channel assignment

4.4 Pulse Receiver

Each heart rate monitor is accompanied with its own pulse receiver. By the reason of receiver diversity from each manufacturer, e.g. transmitter frequency, encoding, a general pulse transmitter is developed by ZMK UNI-KL. The hardware design of pulse receiver will be integrated along with sensor and its circuitry.

The important component in this receiver is an inductor which receives electromagnetic signal from transmitter. First, the signal will amplified about 1000 times. This high amplifier also works as high pass filter with 3.5 kHz cutoff frequency. Afterwards the signal is passed through a low pass filter with cutoff-frequency 5.6 kHz and at the same time will be amplified 81 times.

At the end the signal is passed through a dual monoflops. The output of first monoflop is connected to second one which functioned as a Schmitt trigger. The Schmitt trigger is a comparator application which switches the output negative when the input passes upward through a positive reference voltage. The output second monoflop is connected to reset pin of first monoflop and disable it for 200ms. After the period is running the first monoflop will be retriggered and enabled for reading next pulse. The mechanism of retriggering will solve the problem for encoded pulse transmitter, for example pulse transmitter from Polar.

The output signal from pulse receiver is connected to digital input (pin INT0) on MICAz connector.

4.5 Power Supply

Power supply must provide all components with their specific supply voltage. Because the hardware is designed for a mobile application, rechargeable battery is preferable as power supply.

Power supply circuitry must provide all components with their level of voltage supply. For example, instruments amplifier INA114 which is used to amplify sensor output needs +5V and -5V as supply. Reference temperature sensor IC TMP01 needs +5V, while MICAz is operated with 2x AA batteries with voltage 2.7-3.6V.

We will begin from replacing the 2xAA batteries for MICAz with rechargeable 9V battery. After applying voltage regulator IC 7805 we will get a stable 5V signal. MICAz node needs a stable supply voltage of 2.7–3.3 V, therefore three 1N4007 diodes are used to decrease the voltage to 2.95 Volt. To provide negative voltage supply for the amplifier, ICL7660 negative voltage inverter will be used. It will generate -5V from +5V voltage source.

In Figure 12, the above explained power supply components are drawn as a block diagram.

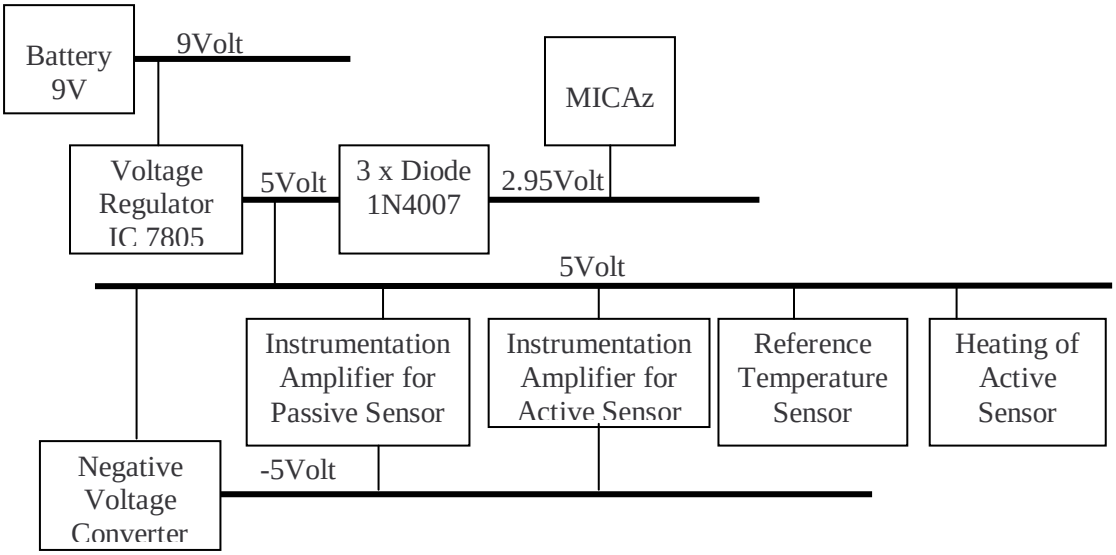

Figure 12: Block diagram for power supply

4.6 Layout and Circuit Board

Described hardware components consisting of sensors, amplifiers, pulse receiver, power supply and the MICAz node must be integrated into a small and compact circuit board. The connection among components is shown as block diagram in Figure 13. Next process, designing the Printed Circuit Board (PCB) will follow the connections on this block diagram.

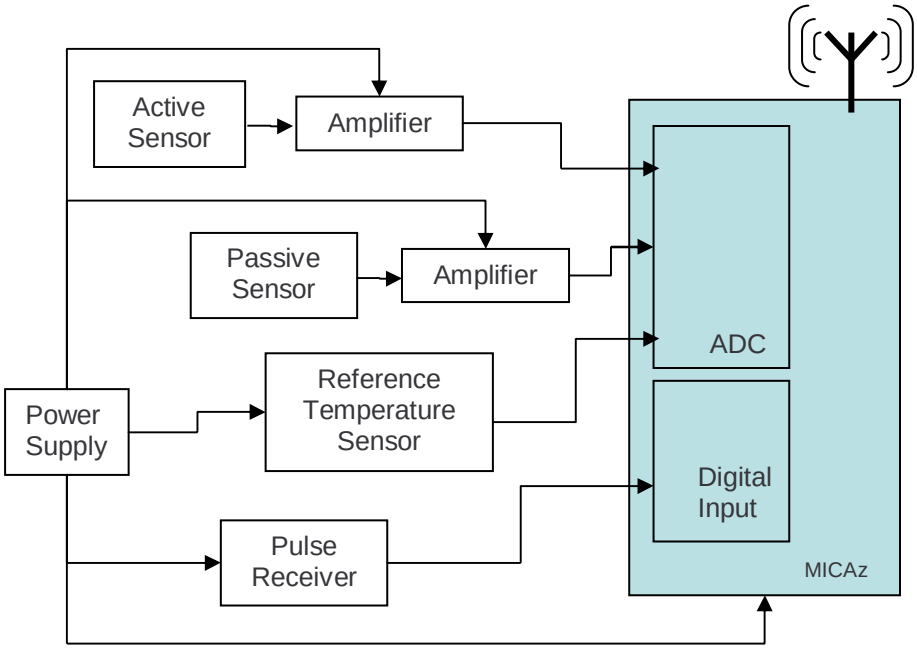

Figure 13: Connection of hardware components

Layout and circuit board which integrates all sensors and its circuitry is drawn using Eagle Layout Editor, a tool for development of Printed Circuit Board. The Printed Circuit Board (PCB) which is developed has size of 6.5 cm x 5.5 cm, and two layers. At bottom the layer, the MICAz is attached using 51 pins Hirose connector. Figure 14 and 15 show the designed circuit board and its layout, respectively.

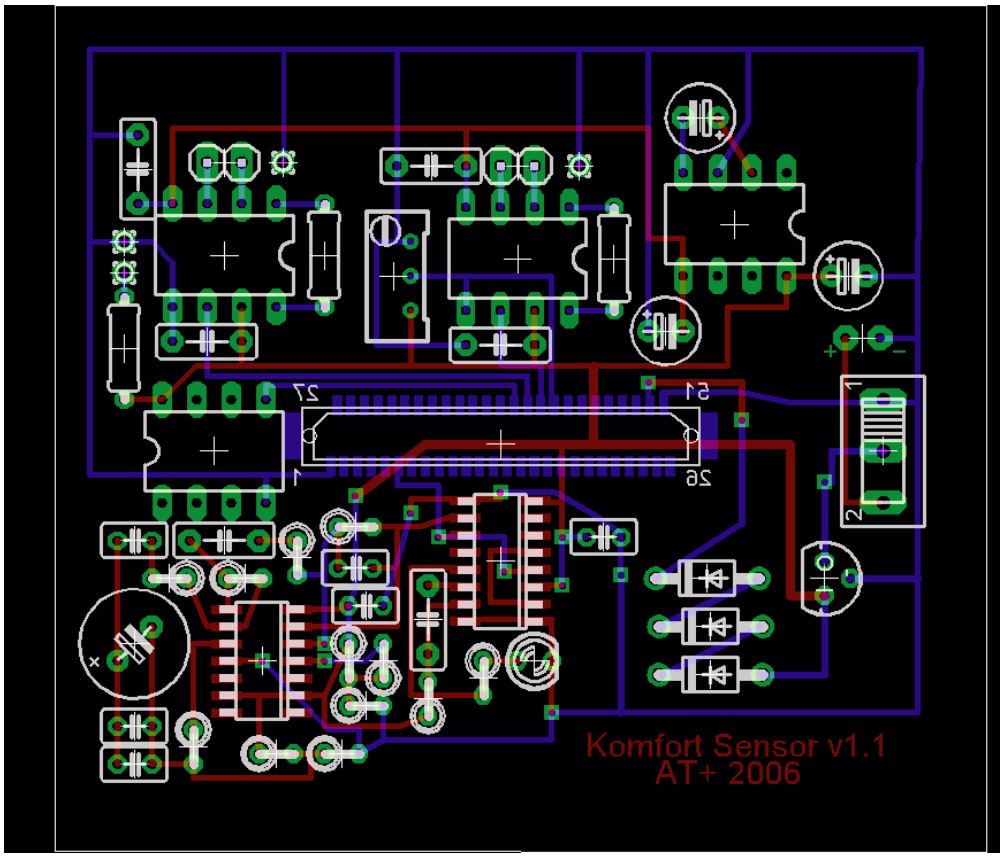

Figure 14: Designed printed circuit board with two layers

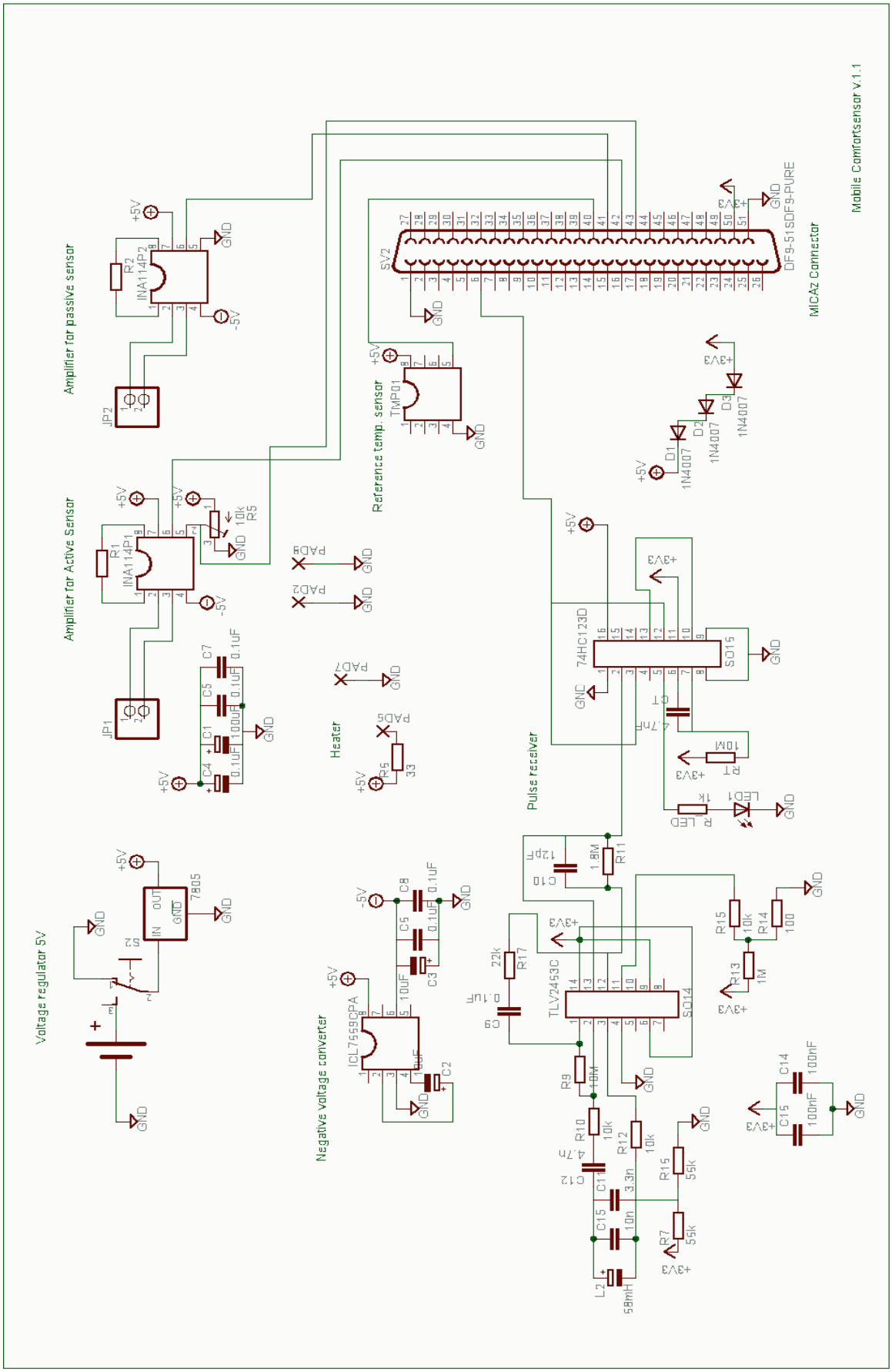

Figure 15: Layout of all hardware components

5 Software Design

5.1 Structure of Communication System

In this chapter, the design of software for the system including sensor board with an attached MICAz and a computer as Graphical User Interface will be introduced. The structure of communication system between sensor boards and the computer is explained as block diagram in Figure 16 below:

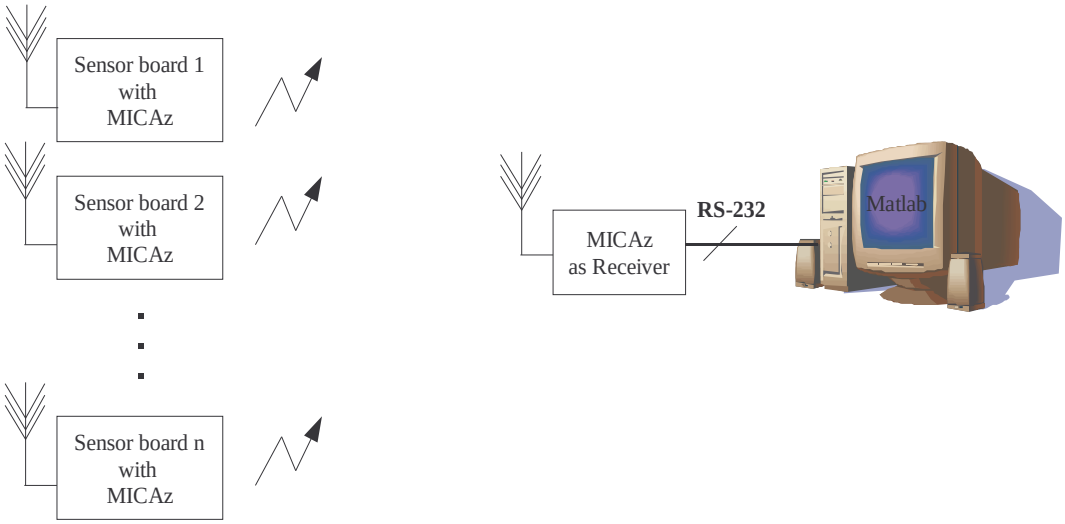

Figure 16: Block diagram of communication system

MICAz nodes which attached to sensor board reads the output of sensors, and runs analog to digital conversion and then sends the data wirelessly to another MICAz node which serves as the receiver. This base station is connected to a computer through a RS-232 cable. A Matlab program will continuously request new data from RS-232 within a specific time range and then process the data.

5.2 TinyOS

For the software development of MICA platform, a special operating system named TinyOS is available. TinyOS is a small, open source, energy-efficient, software operating system developed by UC Berkeley which supports large scale, self configuring sensor networks. Using TinyOS, a single processor board can be configured to run sensor application and mesh networking radio stack simultaneously.

To get a concept of TinyOS programming some keywords will be explained below [11]:

- nesC
  NesC is a programming language in which TinyOS code is implemented. NesC has a C-like syntax, but also supports TinyOS concurrency model. TinyOS codes consist of system, libraries and application.
- Components

A nesC application consists of one or more **components** linked together to form an executable. A component is either a **module** or **configuration**. Modules provide application code which implement one or more interface. These interfaces are the only point of access to the component and bi-directional. An interface declares a set of functions called **commands** and events. Commands must be implemented by the interface provider. Events must be implemented by the interface user. Configurations are used to assemble other components together, connecting interfaces used by components to interfaces provided by others. This is called **wiring**. Every nesC application is described by a **top-level configuration** that *wires* together the components inside.

- Concurrency model
  NesC defines a concurrency model, based on **tasks** and **hardware event handlers**, and detects **data races** at compile time. TinyOS executes only one application program consisting of selected system components and custom components needed for a single application. There are two threads of execution: **tasks** and **hardware event handlers**. Tasks are functions whose execution is deferred. Once scheduled, they run to completion and do not preempt one another. Hardware event handlers are executed in response to a hardware interrupt. Event handler also runs to completion, but may preempt the execution of a task or other hardware event handler. Commands and events that are executed as part of a hardware event handler must be declared with the **async** keyword.

In this work, the application is named AODV_TemperatureSensor. Its top level configuration, Config, is composed from eleven components as illustrated in Figure 17.

In Configuration, there are three modules used, Main, ApplicationM and AODV_EngineM. Main has only one interface: StdControl which is connected to all StdControl interfaces from other components. StdControl is an interface that controls starting, initialization and stopping of component and its subcomponents. By connecting StdControl interface of component Main to all StdControl interfaces of other components, the control of starting, initialization or stopping of all components will be happened at the same time.

The second module, ApplicationM which is implemented in this work, uses nine interfaces, five of them are ADC interfaces and the rest are Timer, Leds, ADCControl and AODVInterface. The ADC interface is a collection of functions: command getData, command getDataContinuously and event DataReady, and is implemented in ADCM module, a part of TinyOS system modules. Commands getData and getDataContinuously initiate an ADC conversion on a given port and a series of ADC conversions, respectively. The event DataReady indicates a sample has been recorded by the ADC as the result of a getData command.

The AODVInterfaces consist of functions which are responsible for sending and receiving data through radio communication and UART, and also functioned as a routing engine. Using AODV (AdHoc on Demand Distance-Vector) routing engine, the connections among network's member, in this case MICAz nodes, will be

constructed after an assignation (on demand). The algorithm is implemented in the last module, AODV_EngineM, which is result of a student research project. For more details of AODV Routing Engine please refer to [Gab04].

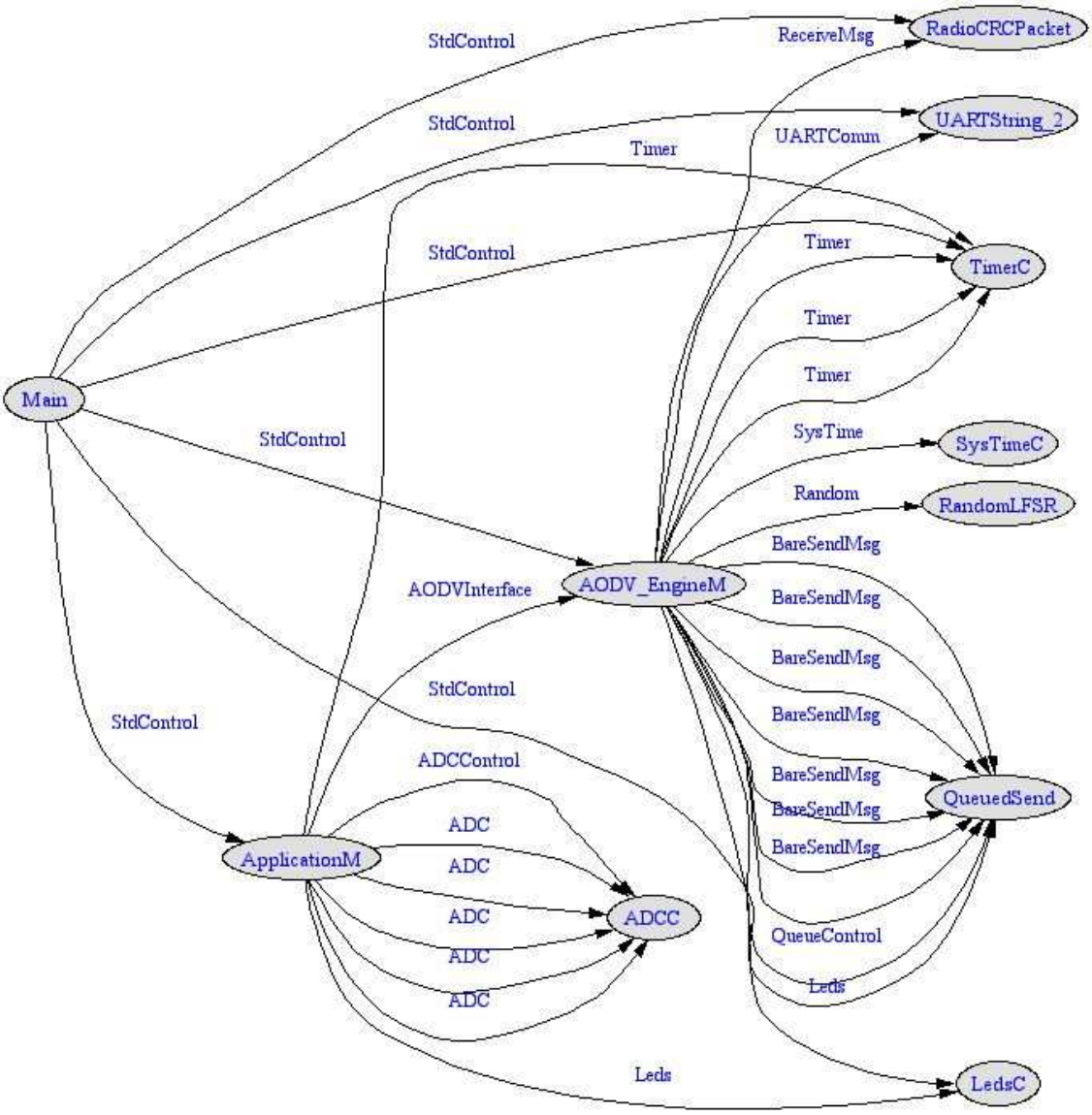

Figure 17: Overview of interface relationship in Configuration file, Config

5.3 Matlab Program

As illustrated before (Figure 16), data from each sensor board is sent to a base station which is connected to a computer through a RS-232 cable. On the computer, a Matlab Simulink program collects and processes the incoming data. Simulink program is divided to three main block diagrams: serial_comm, conversion to physical values, and PMV calculation (see Figure 18).

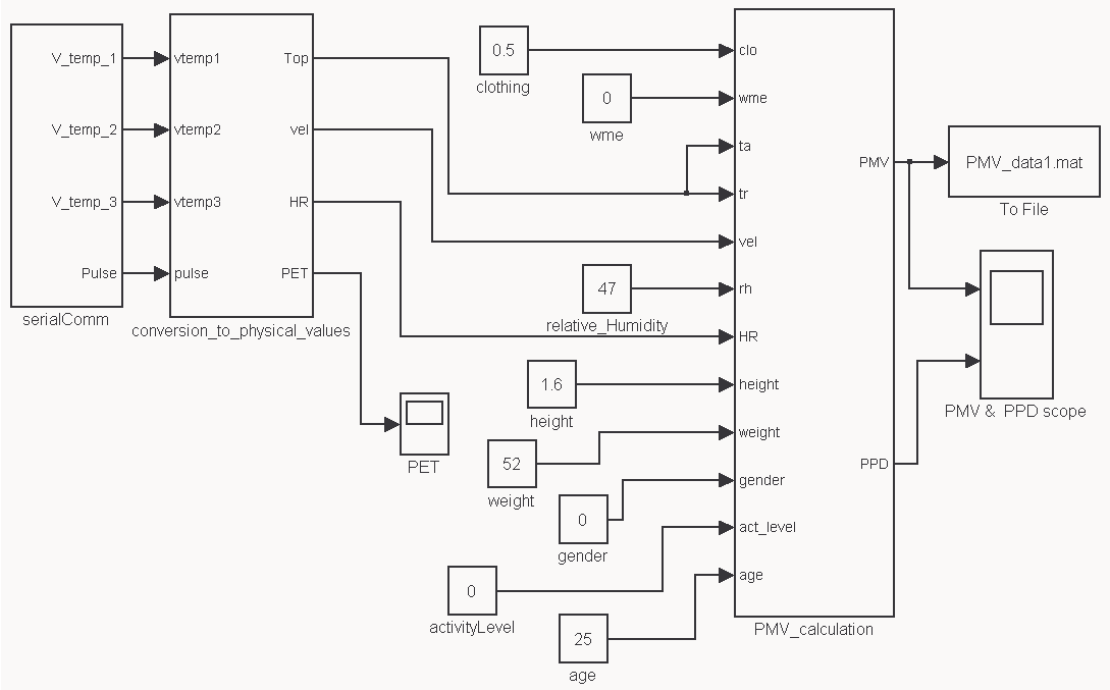

Figure 18: Simulink program

In serial_comm (see Figure 19), telegram from a MICAz node will be read by UART and separated by its index which points to certain information. The telegram consist the information of identity of each node (ID), ADC values which represent voltage of each sensor, pulse from pulse receiver, and two indicators for transmission quality: Received Strength Signal Indicator (RSSI) and Link Quality Indicator (LQI).

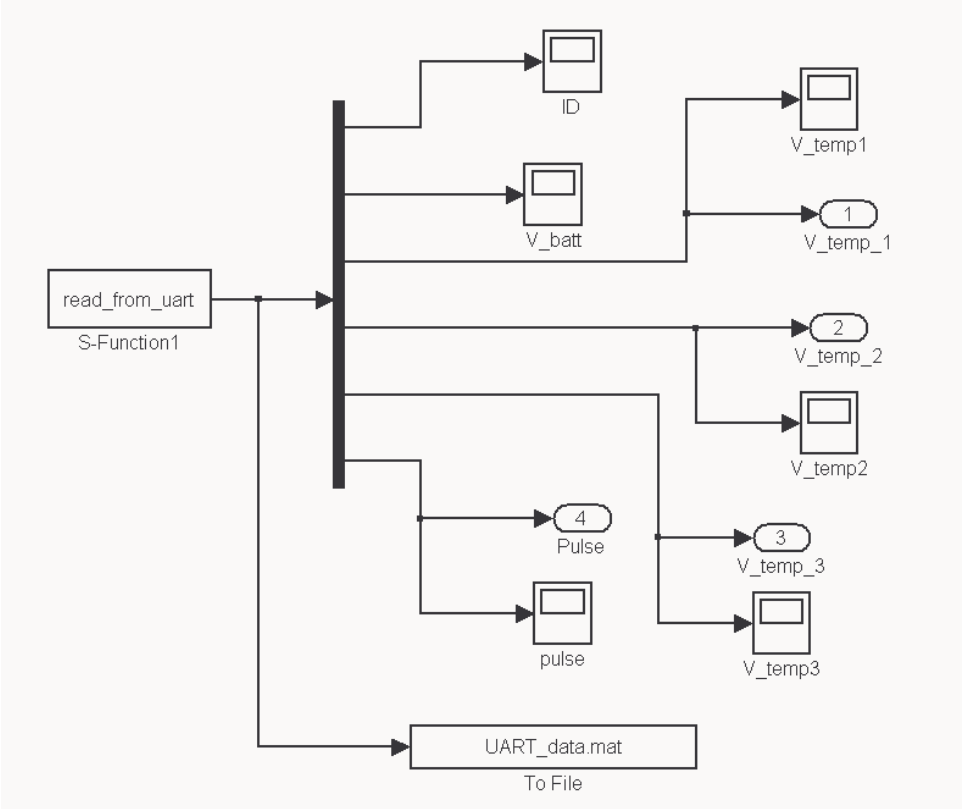

Figure 19: Serial_comm Simulink block diagram

In next block diagram, the ADC values will be converted from digital to its physical meaning.

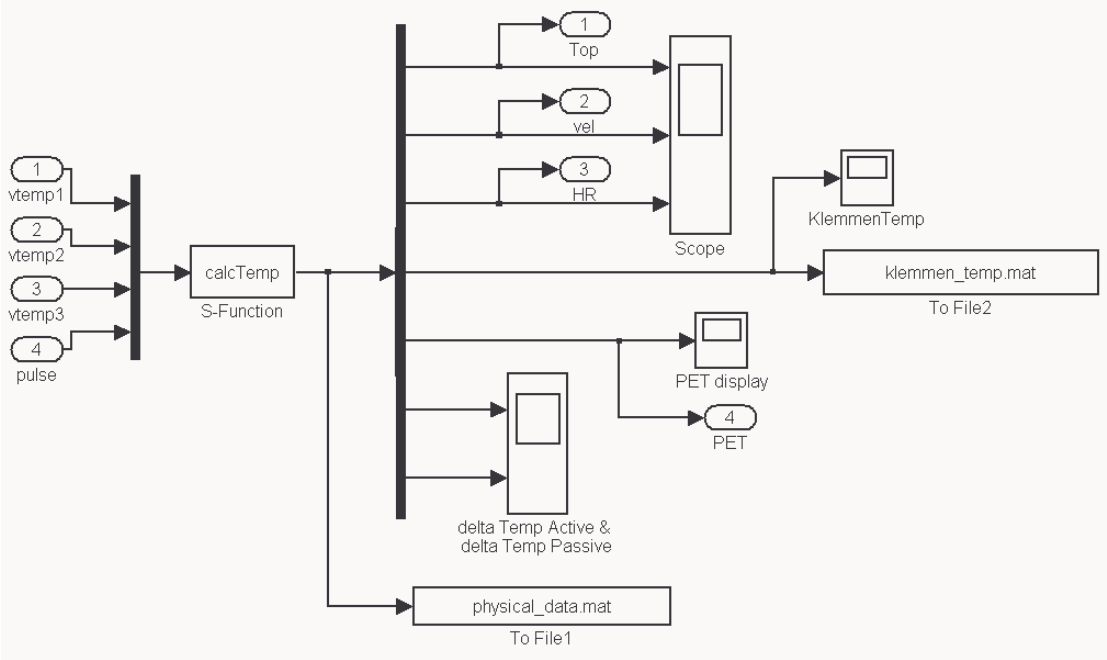

Figure 20: Conversion_to_physical_values_1 Simulink block diagram

And finally in the last block diagram, thermal comfort index is calculated.

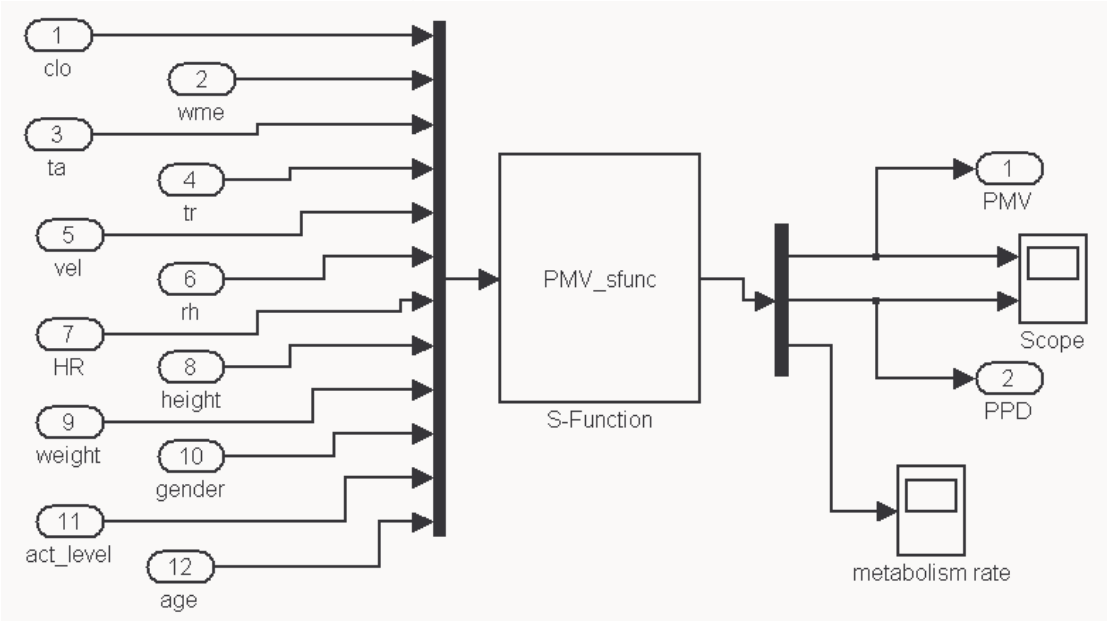

Figure 21: PMV_calculation Simulink block diagram

6 Localization

6.1 Localization Methods

The goal of localization in this work is finding the position of sensor in a wireless network. This process has no influence on PMV calculation, but it will give benefit which makes PMV mapping inside an area possible.

The first step is to collect some localization methods and select a method which is mostly suitable for this application. Some localization systems that are implemented using wireless sensor networks are listed below [Ter06]:

- Beacon-based localization, UCLA, 2000
  The system used five radio packet controller modules. Four of these modules were placed in corners of a 10x10 meter outdoor region. These modules, or beacons, served as reference points and continuously transmitted packets with their unique ID every two seconds. The other module was used as a receiver and listened for messages. It decided which modules it was connected based on percentage of message that it received.

- SpotOn, University of Washington, 2001
  SpotOn was created with the idea of ad-hoc location sensing. SpotOn tags are attached to any object to be localized. The tags beacon radio packets of a calibrated power at randomized interval. The tags measure the received signal strength indicator (RSSI) upon hearing beacons. A receiver-specific calibration model is used with the RSSI to estimate the distance from the transmitting node. Placing a transmitter 50 centimeters from the note to be calibrated and having it transmit 100 packets accomplished the calibration. Object can be located relative to another object, or some objects can be used to leverage the location data.

- Calamari, University of California Berkeley, 2002.
  Calamari system was built with MICA sensors and estimates the distance between nodes by RSSI and acoustic time of flight (TOF) measurements. The TOF hardware has drawback of consuming more power as well as the additional cost of special hardware. The advantage is that this technique yields more accurate distance estimates than by RSSI alone.

The latest localization system is developed by is Western Michigan University. The system, Ferret, was also built with MICA nodes and implied two techniques: potentiometer measurement and RSSI measurement. In order to localize, the system must be able to established relationship between distance notes and radio property, either potentiometer or RSSI value [Höp99]. This relationship varies among different environments due to interference from machinery, indoors vs. outdoors, etc. When the Ferret system is moved to another environment, the relationship must be renewed.

In the potentiometer technique, the object to be located (the mobile node) begins to transmit the beacon at the lowest power level and waits for replies from infrastructure nodes. The power level is increased with each transmission until the mobile node gets

three replies. These replies are then forwarded to a base station to compute the position based on triangulation method.
The RSSI method can be applied after the relationship between distance and RSSI is known. Therefore, some experiments must be performed first to estimate the distance based on RSSI. In RSSI method, the mobile node sends out a series of five signals using full transmission power. The infrastructure nodes reply to all beacons that they heard. The mobile node records identification number and RSSI from all infrastructure nodes. It then computes the average RSSI for each neighbor and identifies three closest neighbors by the largest RSSI average. Thereafter, the data is forwarded to a base station which will perform location calculation.

6.2 RSSI Measurement

After comparing the localization methods above and the fact that we already use MICAz to transmit data, it is proposed to select the RSSI measurement method to perform the localization. No additional hardware is needed because RSSI value is automatically sent by transmitting.

Thereafter, a simple measurement has been done to check whether this method is applicable. The measurement is conducted in Room 12-471 which the walls are from metal using two MICAs. Both of MICAz are placed on the table. One MICAz which acts as sender transmits the dummy data to another MICA which acts as receiver. The receiver is placed in the same position (position 1 on Figure 22) during all measurements, while the sender is moved forward 50 cm each after 16 transmissions. Below are figures of measurement configurations and their RSSI values:

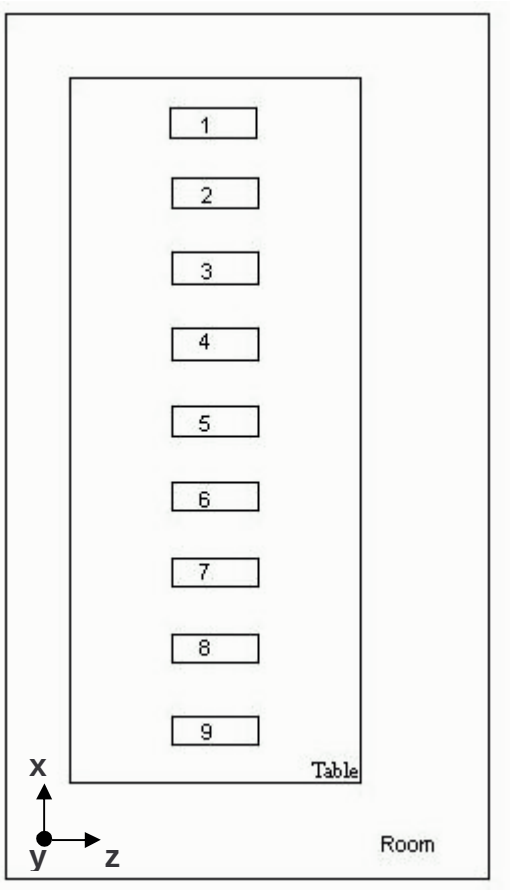

Figure 22: Positions of sender in configuration 1

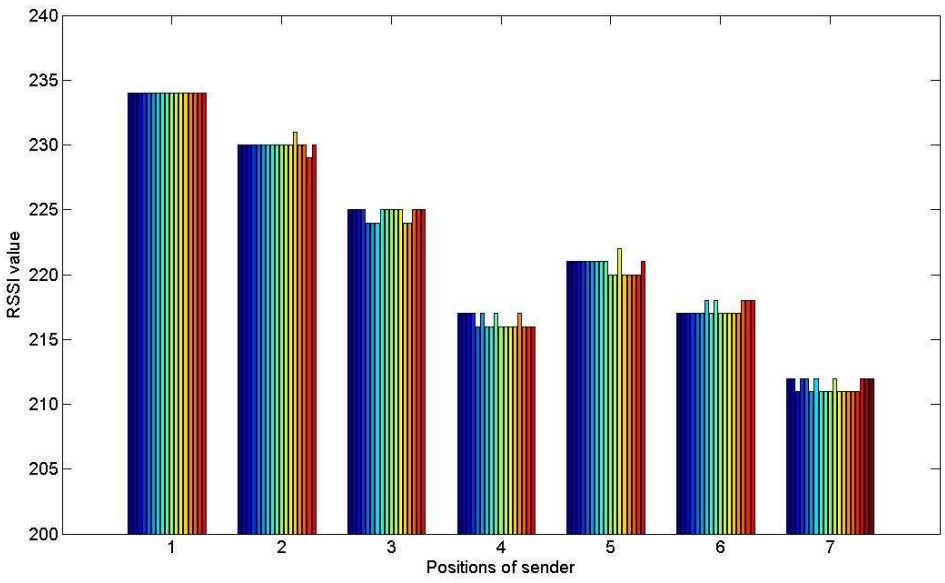

Figure 23: RSSI for configuration 1

The result showed that RSSI value has no linear relationship with distance in this room. Therefore we cannot use this relationship alone to gain location information.

Next measurement is conducted in the same room, with different configuration of sender and receiver. This time, the aim is only to locate some important points in the room, which is where the people seat (location of chairs). The sender configuration and results can be seen in Figure 24, 25 and 26.

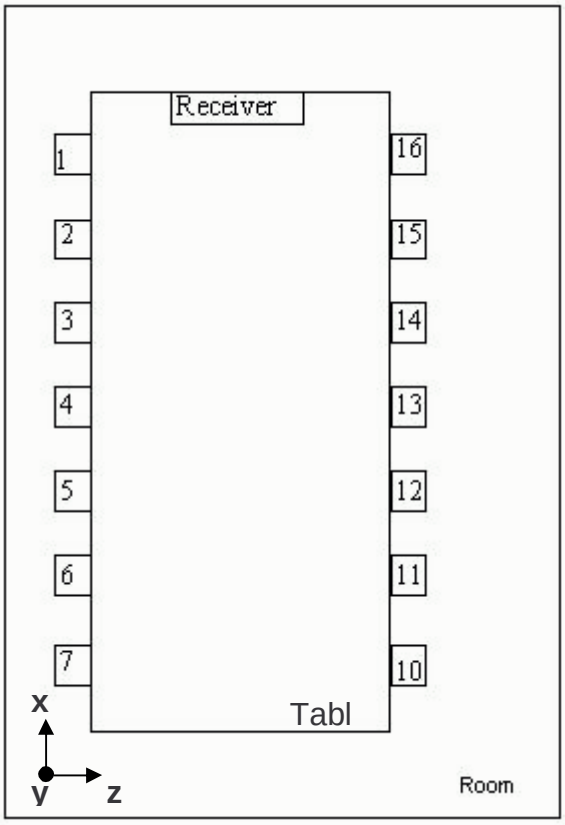

Figure 24: Positions of sender in configuration 2

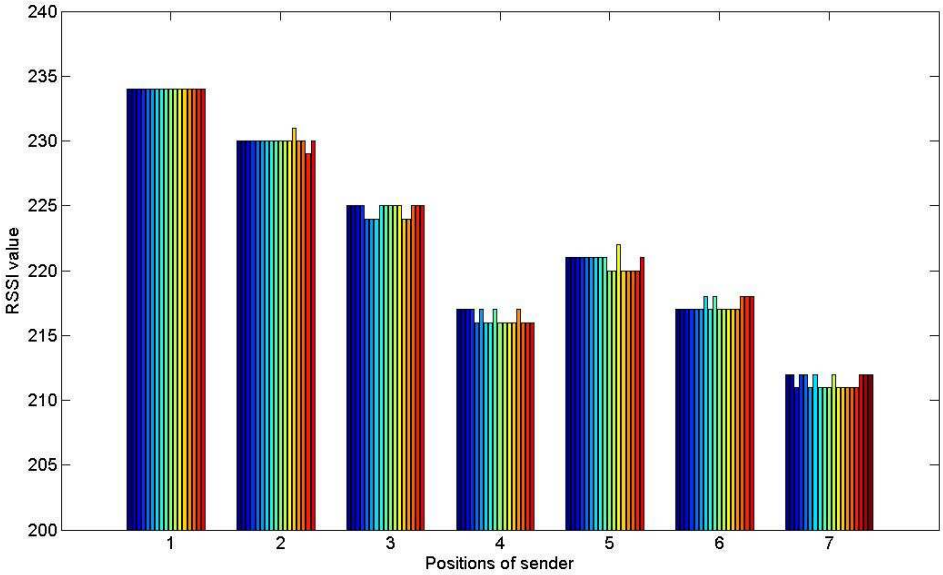

Figure 25: RSSI from configuration 2, positions 1 – 7

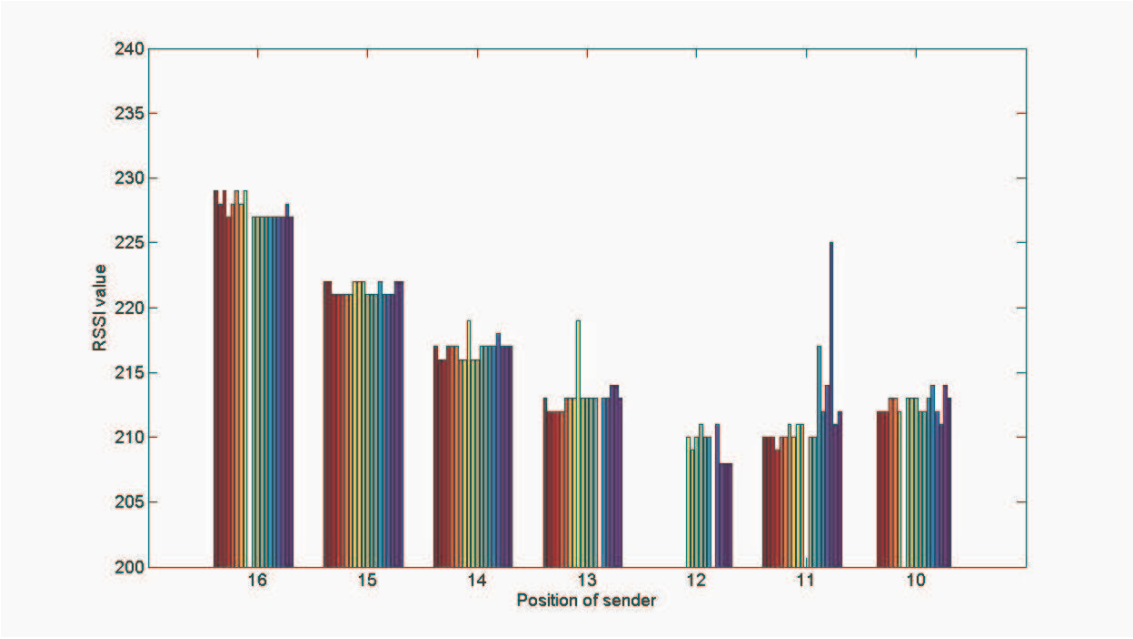

Figure 26: RSSI from configuration 2, positions 10 - 16

Based on experiments result, it can be concluded that location of chairs cannot be gained by using only one receiver.

Next measurement is taken by using two receivers as illustrated in Figure 27. Each sender transmits simultaneously data to both receivers. RSSI from Receiver 1 with sender position 1-7 is shown in Figure 28, and from receiver 2 with sender position 1-7 is shown in Figure 29.

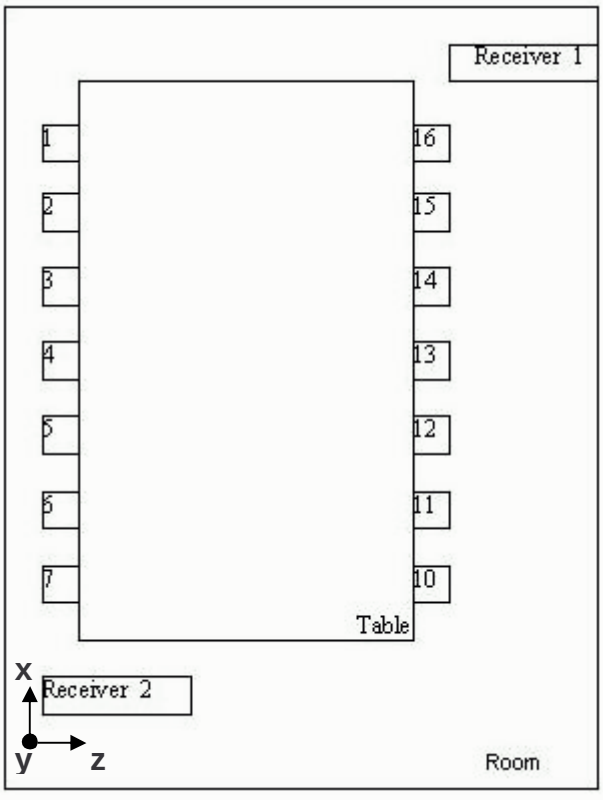

Figure 27: Proposed configuration with two receivers

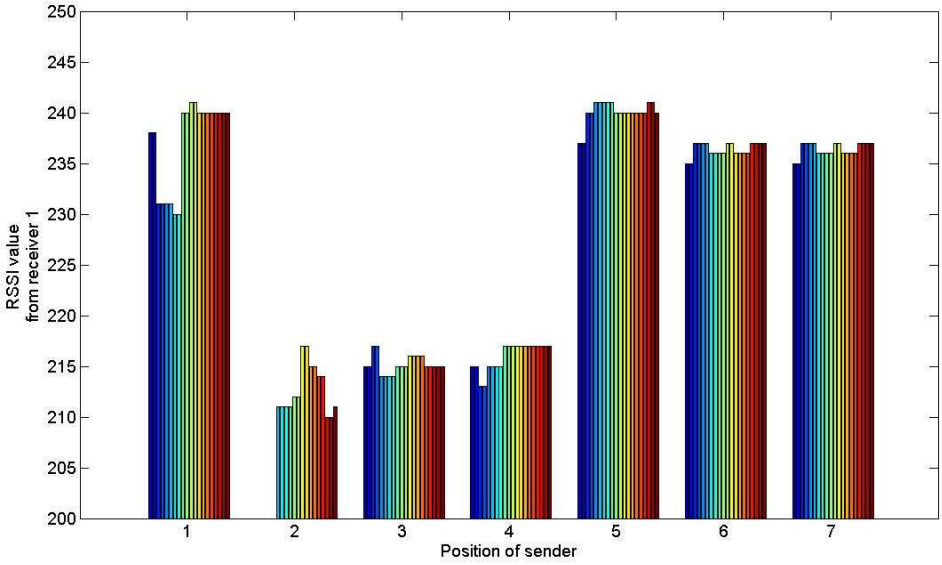

Figure 28: RSSI from receiver 1

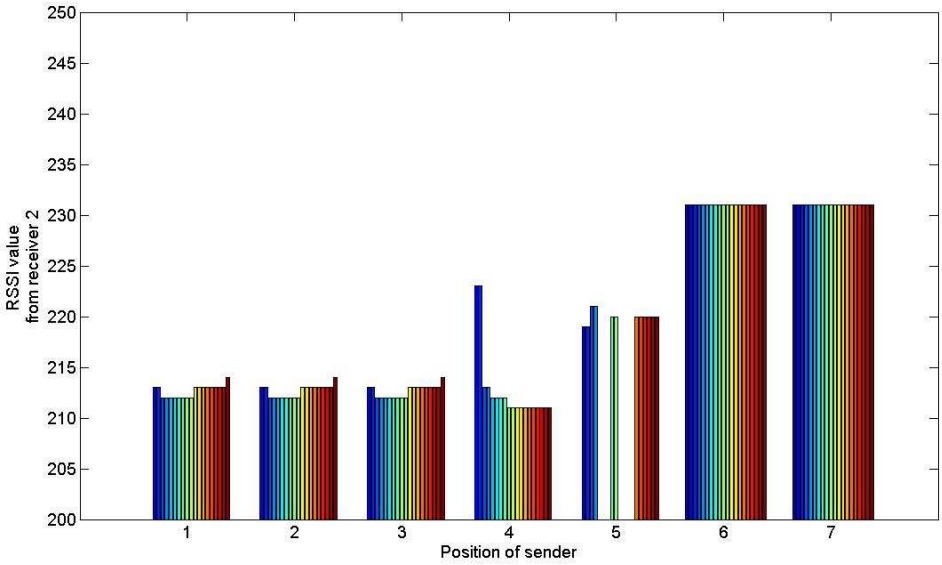

Figure 29: RSSI from receiver 2

With two receivers, it is not possible to distinguish among location 2, 3 and 4, because the RSSI pairs which are produced from each location are quite similar. The same problem happened with position 6 and 7. To solve this problem it is suggested to use three or more receivers.

7 Measurement Results

7.1 Experimental Setup

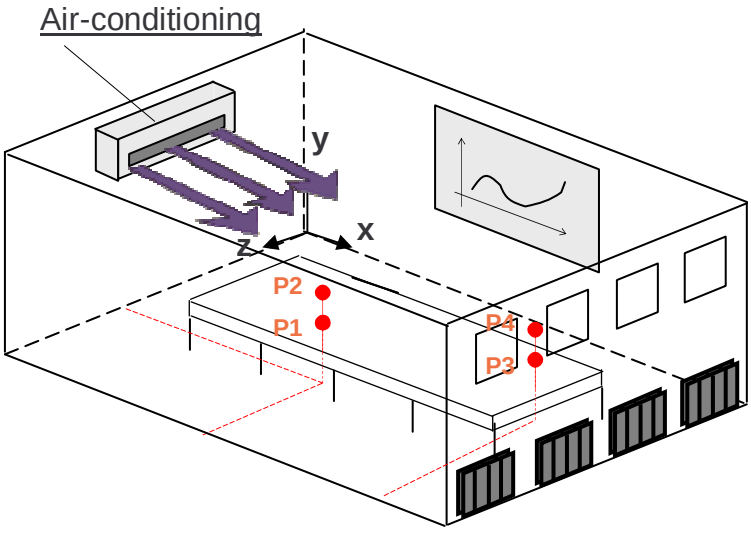

Figure 30: Measurement points at conference room, University of Kaiserslautern

The PMV measurement was taken at a conference room at the University of Kaiserslautern (Figure 30). The room is air conditioned with three possibilities of controller manipulator: air-conditioner, heating and windows. In this measurement, we will investigate some effects of cooling and ventilation by air-conditioner only. The heating is set off and the windows are closed.

As seen in the Figure 30, there are four selected measurement points, P1, P2, P3 and P4. Point P1 has coordinate x = 3.56 m, y = 1.20 m, z = 2.81 m. P2 has coordinate x = 3.56 m, y = 1.80 m, z = 2.81 m. P3 has coordinate x = 5.6 m, y = 1.20 m, z = 2.3 m. P4 has coordinate x = 5.6 m, y = 1.80 m, z = 2.3 m. For each point, two measurements are taken, first with ventilation and the second with cooling. The air-conditioners outlet angles for both modes are by 10°. The fan level of air-conditioner is 5 which refer to air mass flow of approximately 0.246 kg/s. The air humidity in the room is by 47%. Each measurement at each point was taken at different time.

The object person for this measurement is a female, 25 years old, 1.6 meter tall, and 52 kg weight and doing a light activity (sitting) of 1.2 met. The person wears light clothing with resistance of 0.5 clo.

Measurement results are shown in Figure 31 until Figure 38. Additionally to PMV, the perceived temperature will also be calculated using equation (14). The perceived temperature is developed from MEMI model and defined as an equivalent air temperature at a reference environment. Based on this model, the perceived temperature will be equivalent to operative room temperature when air velocity is 0.1 m/s.

7.2 Measurement at Point P1, Ventilation Mode

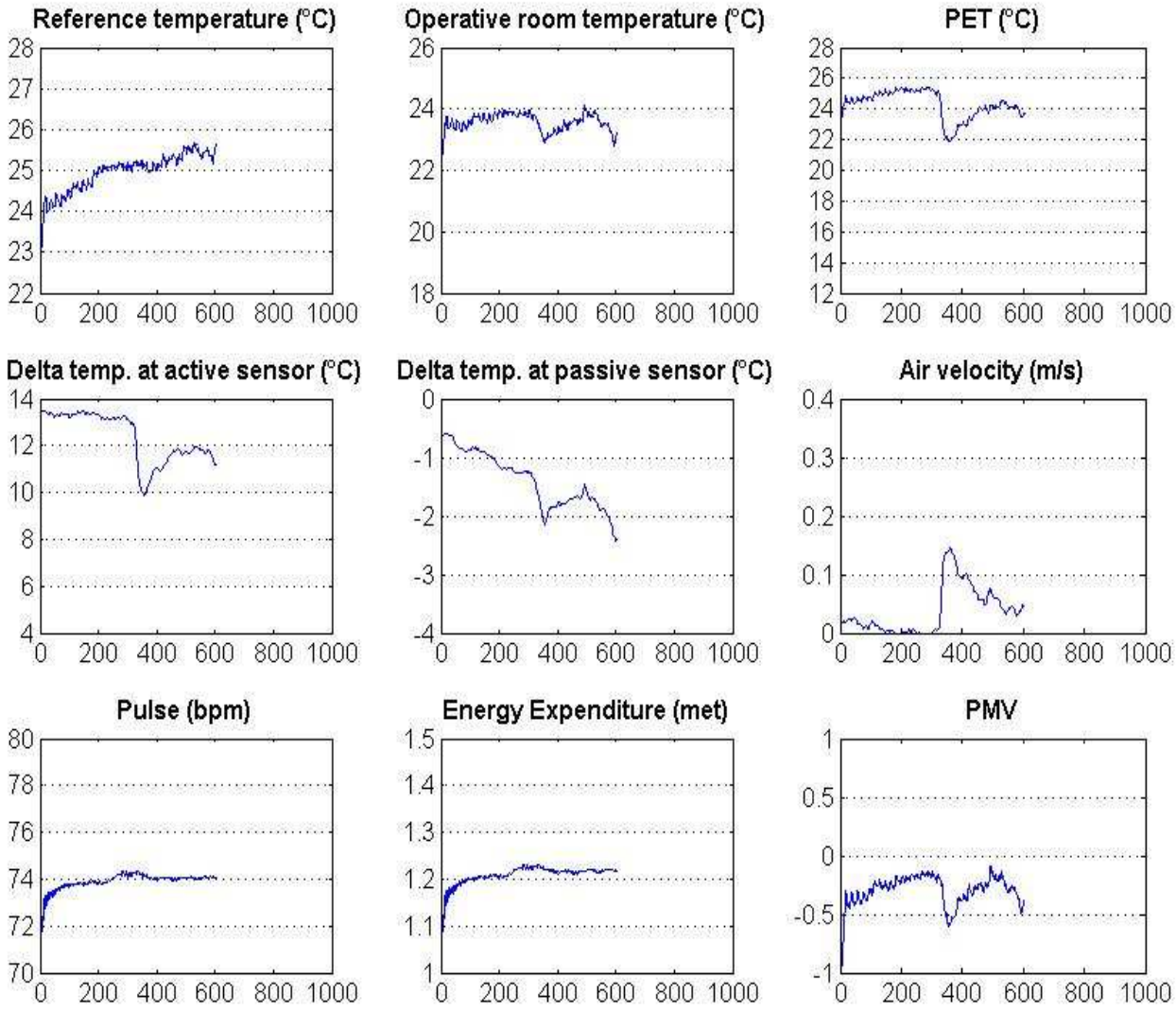

Figure 31: Measurement at point P1, Ventilation mode

Measurement was begun with the air-conditioner off and operative room temperature of 23°C. After 300 seconds, the air-conditioner was switched on to ventilation mode. After switching on temperature at active sensor decreased until 10°C, but then increased again up to 12°C. Measured air velocity is maximum 0.15 m/s. The perceived temperature decreased by 1°C from 25°C before ventilating to 24°C after ventilation. PMV slightly decreased from 0.3 to 0.2 which means the thermal comfort sensation was between neutral to slightly warm.

7.3 Measurement at Point P1, Cooling Mode

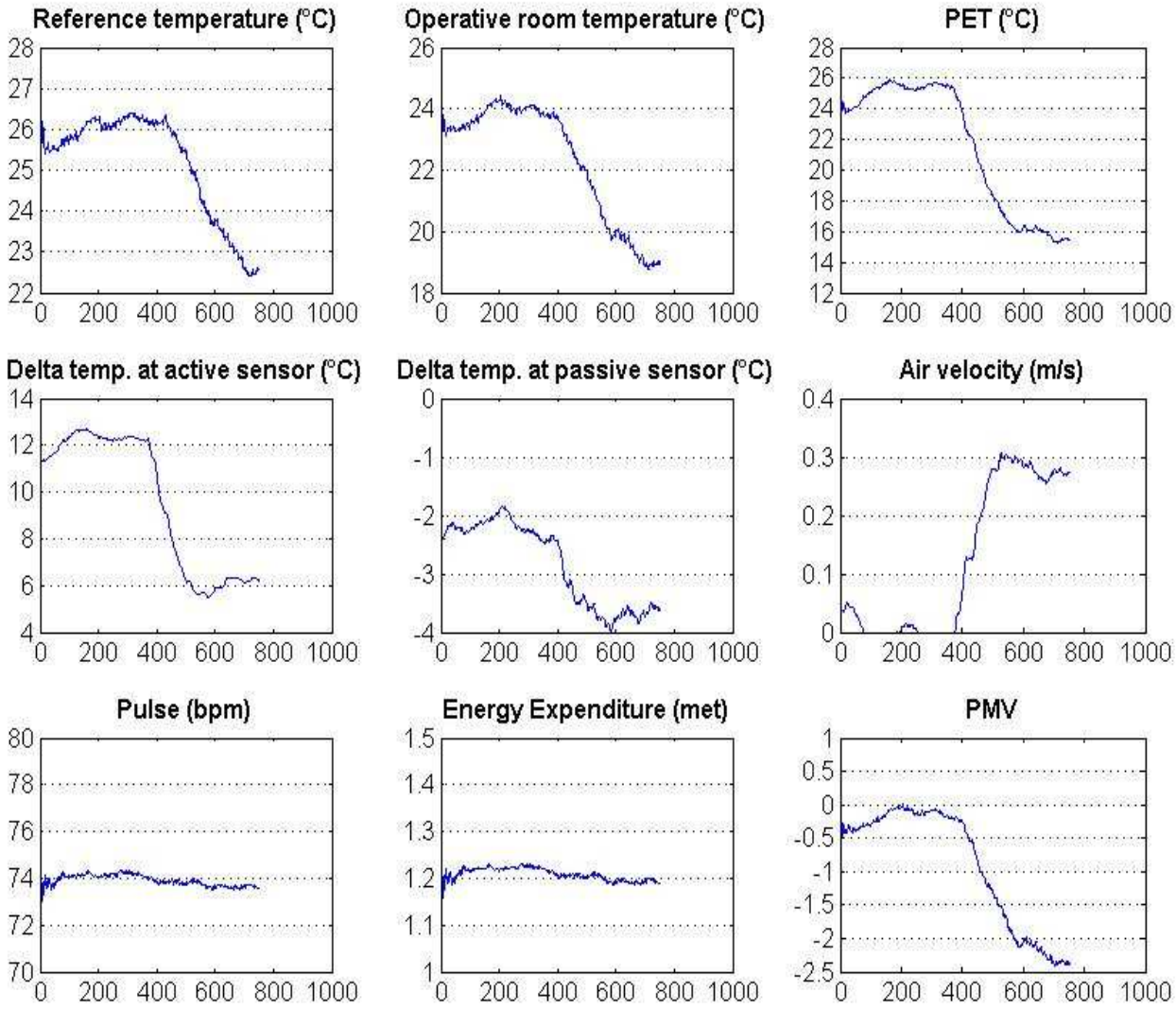

Figure 32: Measurement at point P1, Cooling mode

Measurement was begun with the air-conditioner off and operative room temperature of 23°C. After 330 seconds the air-conditioner was switched on to cooling mode. Delta temperature at active sensor decreased by 6°C, while delta temperature at passive sensor decreased by -4°C. The measured air velocity at this point is 0.3 m/s. Perceived temperature decreased from 26°C to 16°C. PMV decreased from 0.2 (neutral to slightly warm) to -1.5 (slightly cool to cool).

7.4 Measurement at Point P2, Ventilation Mode

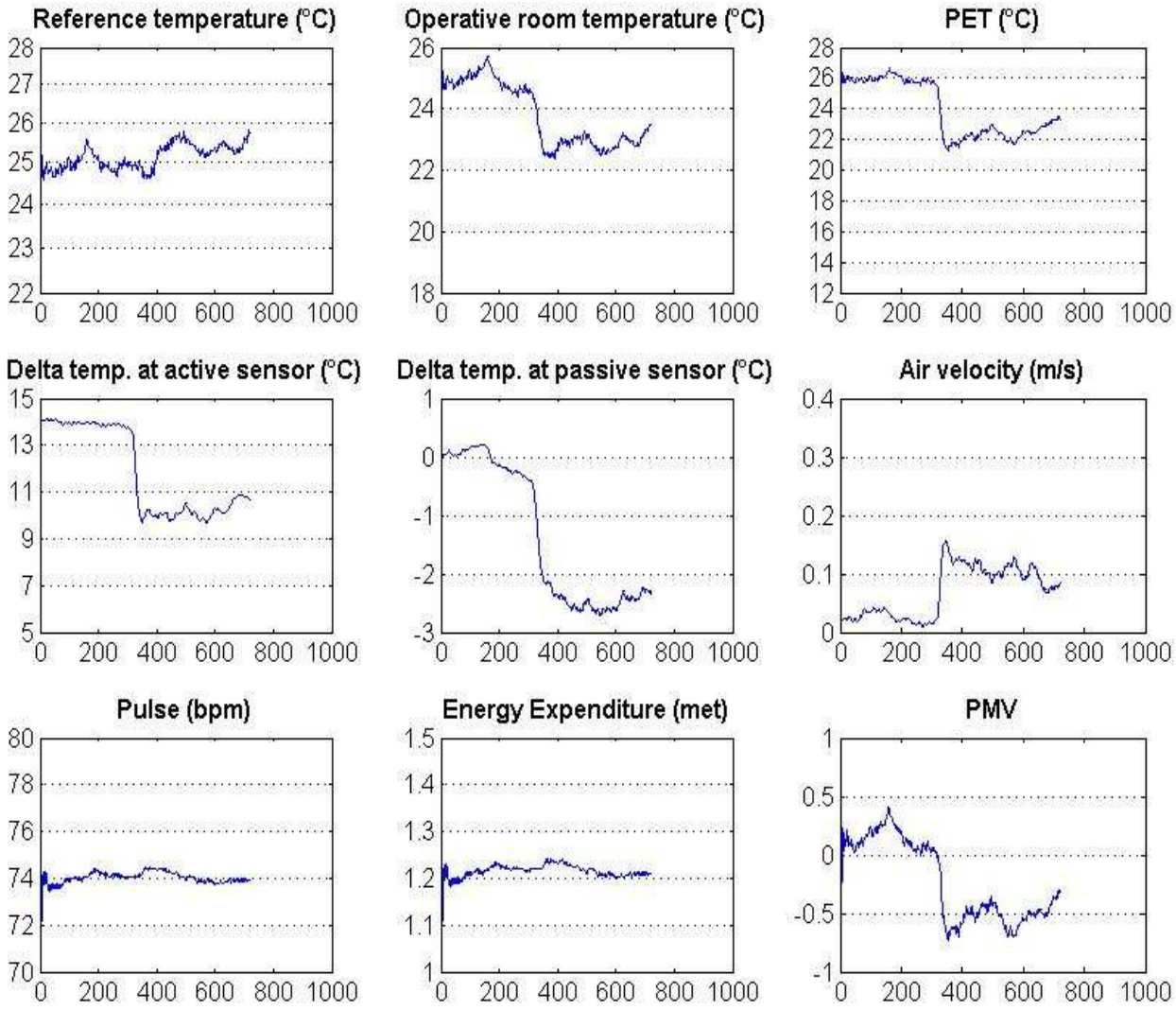

Figure 33: Measurement at point P2, Ventilation mode

Measurement was begun with the air-conditioner off and operative room temperature of 25°C. After 230 seconds the air-conditioner was switched on to ventilation mode. Delta temperature at active sensor decreased from 14°C to 10°C and delta temperature at passive sensor decreased from 0°C to -2.5°C. Operative room temperature decreased about 3°C because the air which flows from the ventilating air conditioner was still slightly cooler than air in the room (from last measurement). Measured air velocity maximum was 0.15 m/s. Perceived temperature decreased from 26°C to 22-23°C. PMV decreased from 0.5 (slightly warm) to 0 (neutral).

7.5 Measurement at Point P2, Cooling Mode

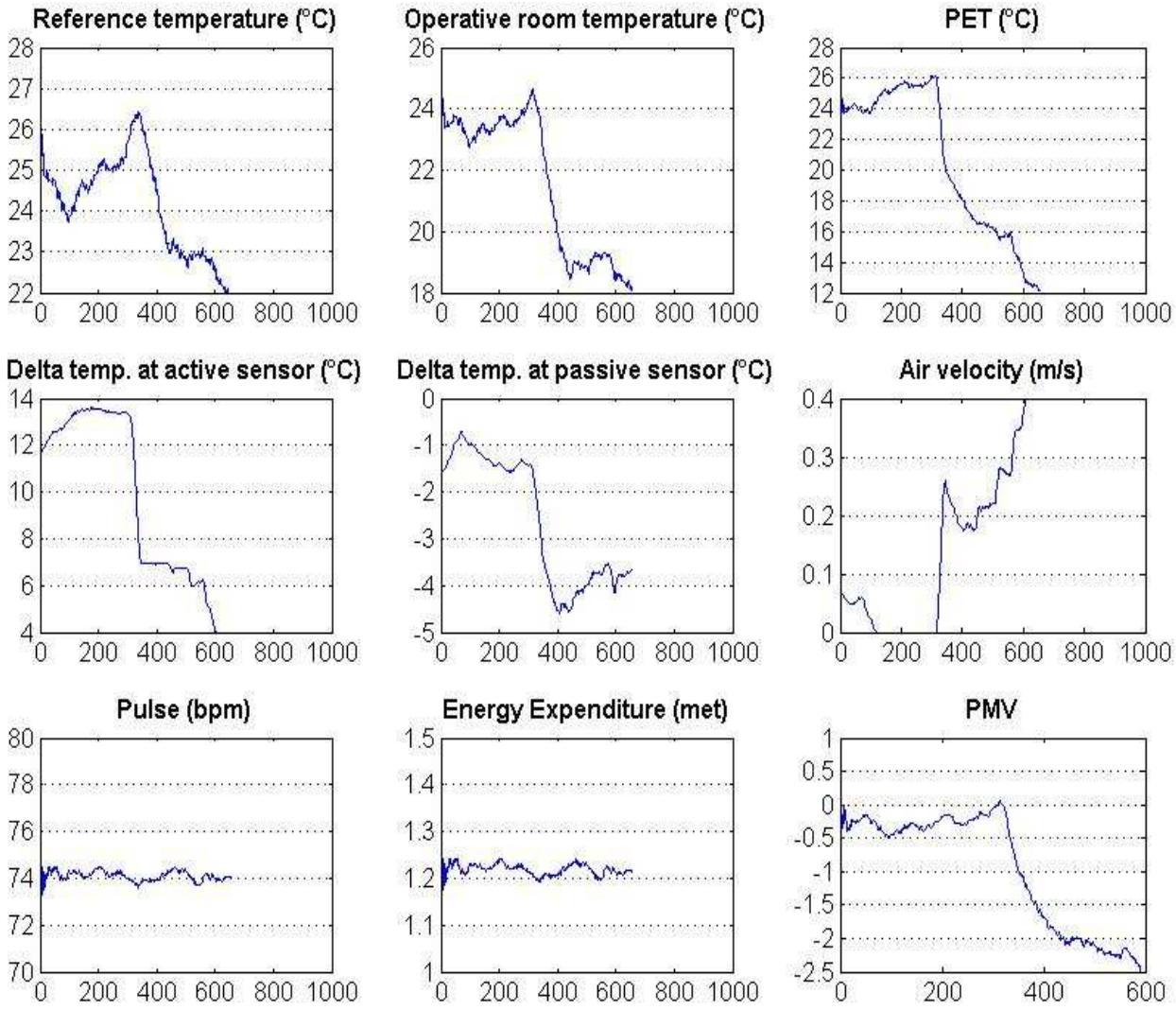

Figure 34: Measurement at point P2, Cooling mode

Measurement was begun with the air-conditioner off and operative room temperature of 24°C. After 240 seconds the air-conditioner was switched on to cooling mode. Delta temperature at active sensor decreased from 13.5°C to 4°C while delta temperature at passive sensor slightly decreased from -1.5°C to -4°C. Maximum measured air velocity was 0.4 m/s. Perceived temperature before cooling was 26°C and after cooling was 12°C. PMV before cooling was 0.5 m/s (slightly warm) and after cooling was -2 (cool).

7.6 Measurement at Point P3, Ventilation Mode

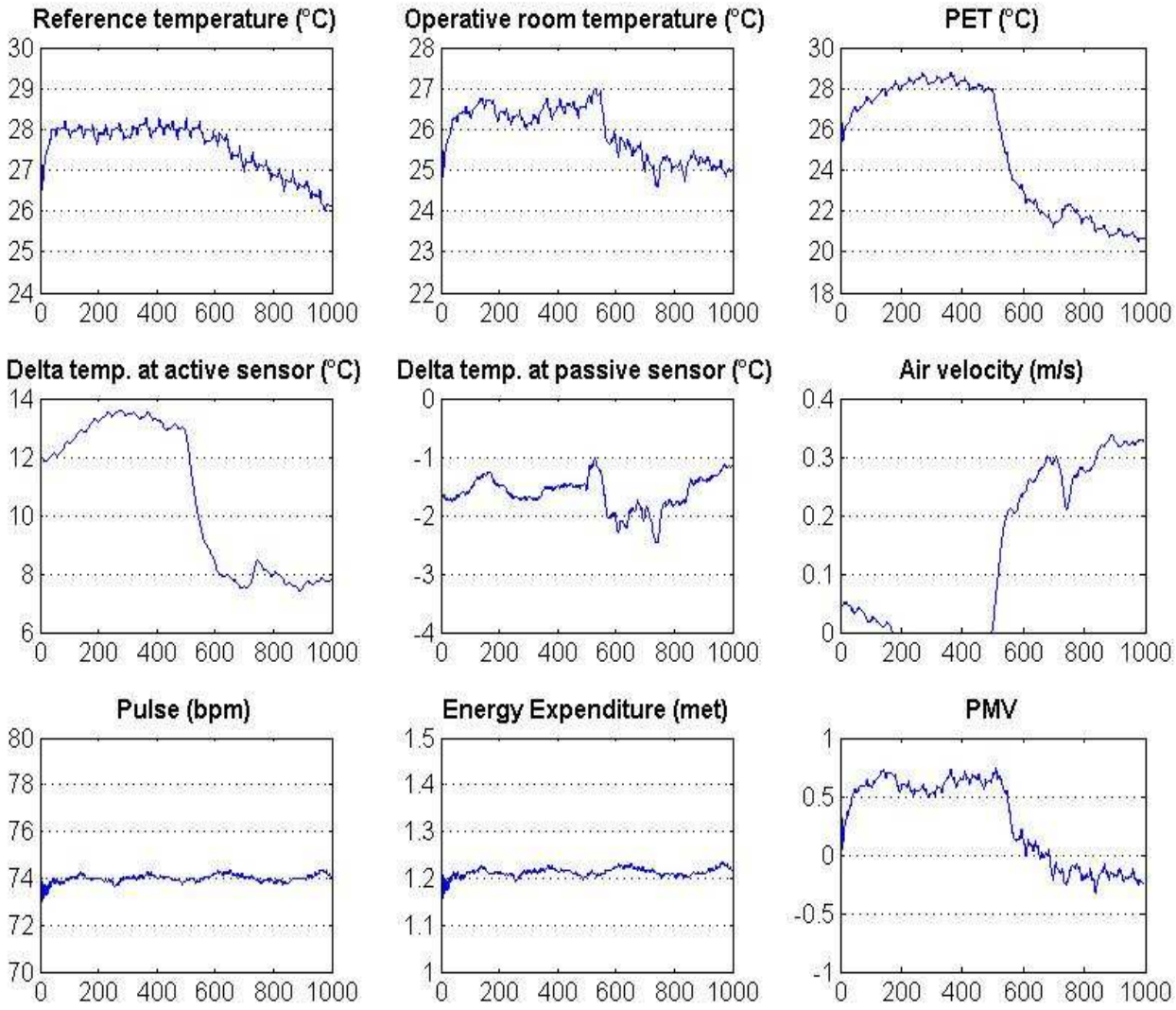

Figure 35: Measurement at point P3, Ventilation mode

Measurement was begun the air-conditioner off and operative room temperature of 26°C. After 480 seconds the air-conditioner was switched on to ventilation mode. Delta temperature at active sensor decreased from 13°C to 8°C. At passive sensor temperature was relative constant. Two degree Celcius decrement of operative room temperature happened because the air which flows from the ventilating air conditioner was cooler than air in the room. The measured air velocity was 0.33 m/s. Perceived temperature was decreased from 28°C to 21°C. PMV before the ventilating was 0.2 and after ventilating was -0.25 (neutral to slightly cool).

During the measurement the air-conditioner was switched on and off twice, at 695 seconds and at 935 seconds. Both changes affected delta temperature at active and passive sensors directly.

7.7 Measurement at Point P3, Cooling Mode

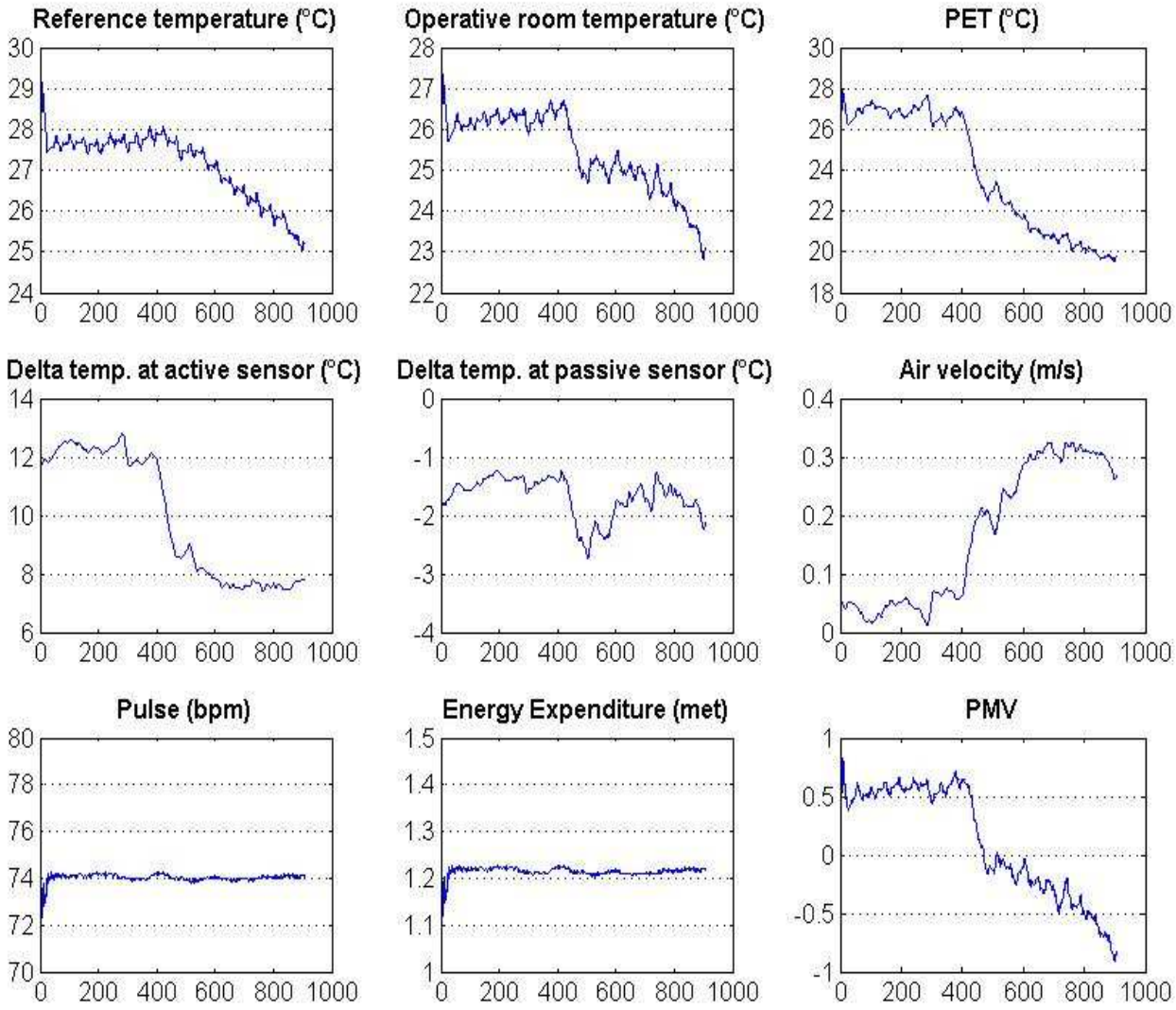

Figure 36: Measurement at Point P3, Cooling mode

Measurement was begun with the air-conditioner off and operative room temperature of 26°C. After 380 seconds the air-conditioner was switched on to cooling mode. After 520 seconds of cooling the operative room temperature decreased to 23°C. Delta temperature at active sensor decreased from 12.5°C to 6°C, and delta temperature at passive sensor decreased from -1°C to -3.5°C. Maximum measured air velocity was 0.32 m/s. The perceived temperature decreased from 27°C to 20°C and PMV decreased from 0.5 to -0.8.

7.8 Measurement at Point P4, Ventilation Mode

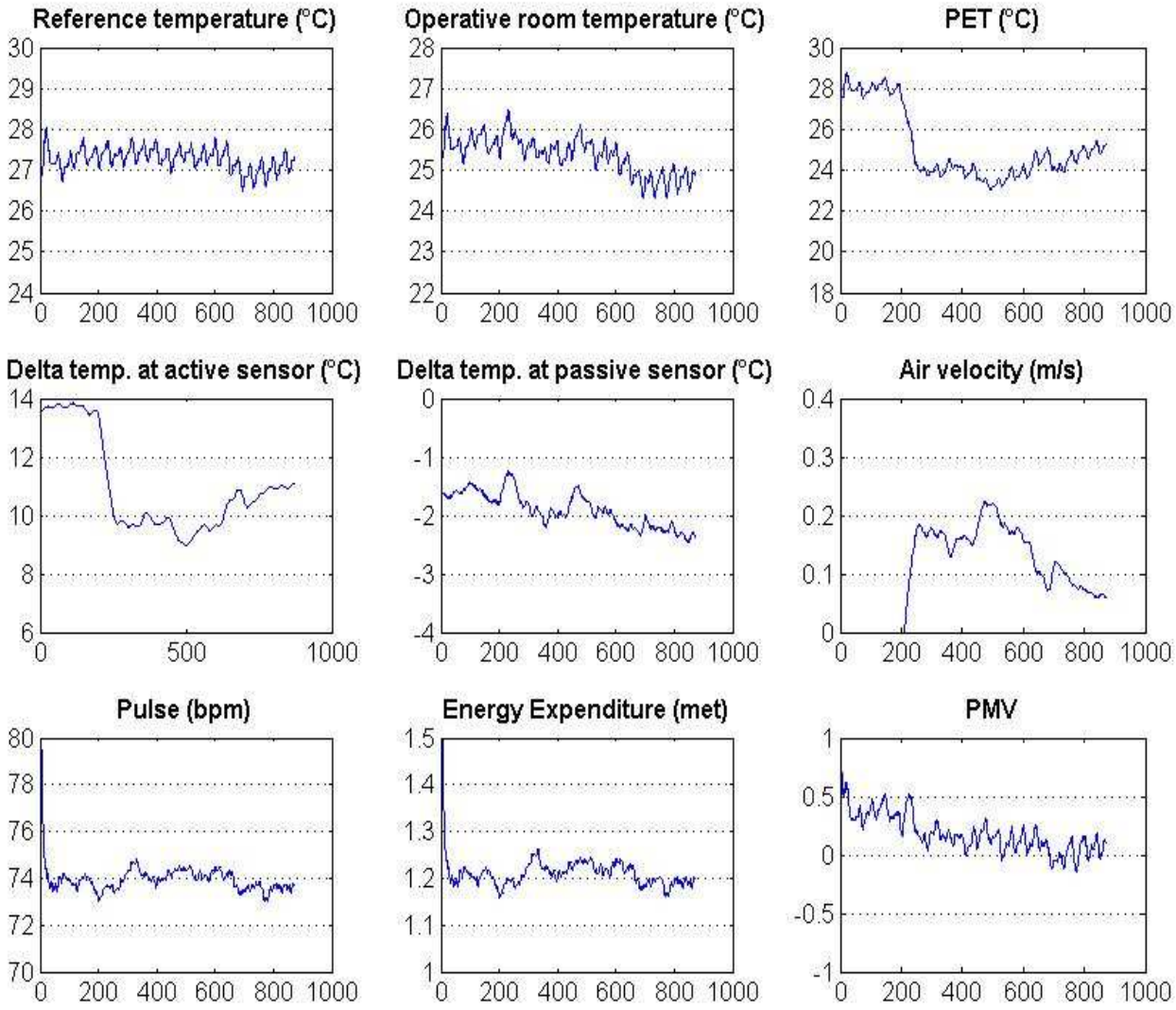

Figure 37: Measurement at point P4, Ventilation mode

Measurement was begun with the air-conditioner off and operative room temperature of 26°C. After 178 seconds the air-conditioner was switched on to ventilation mode. Delta temperature at active sensor decreased from 14°C to 11°C and at passive sensor decreased from -1.5°C to -2.4°C. Measured air temperature was 0.23 m/s. The perceived temperature decreased from 28°C to 25°C. PMV decreased from 0.5 (slightly warm) to 0 (neutral)

7.9 Measurement at Point P4, Cooling Mode

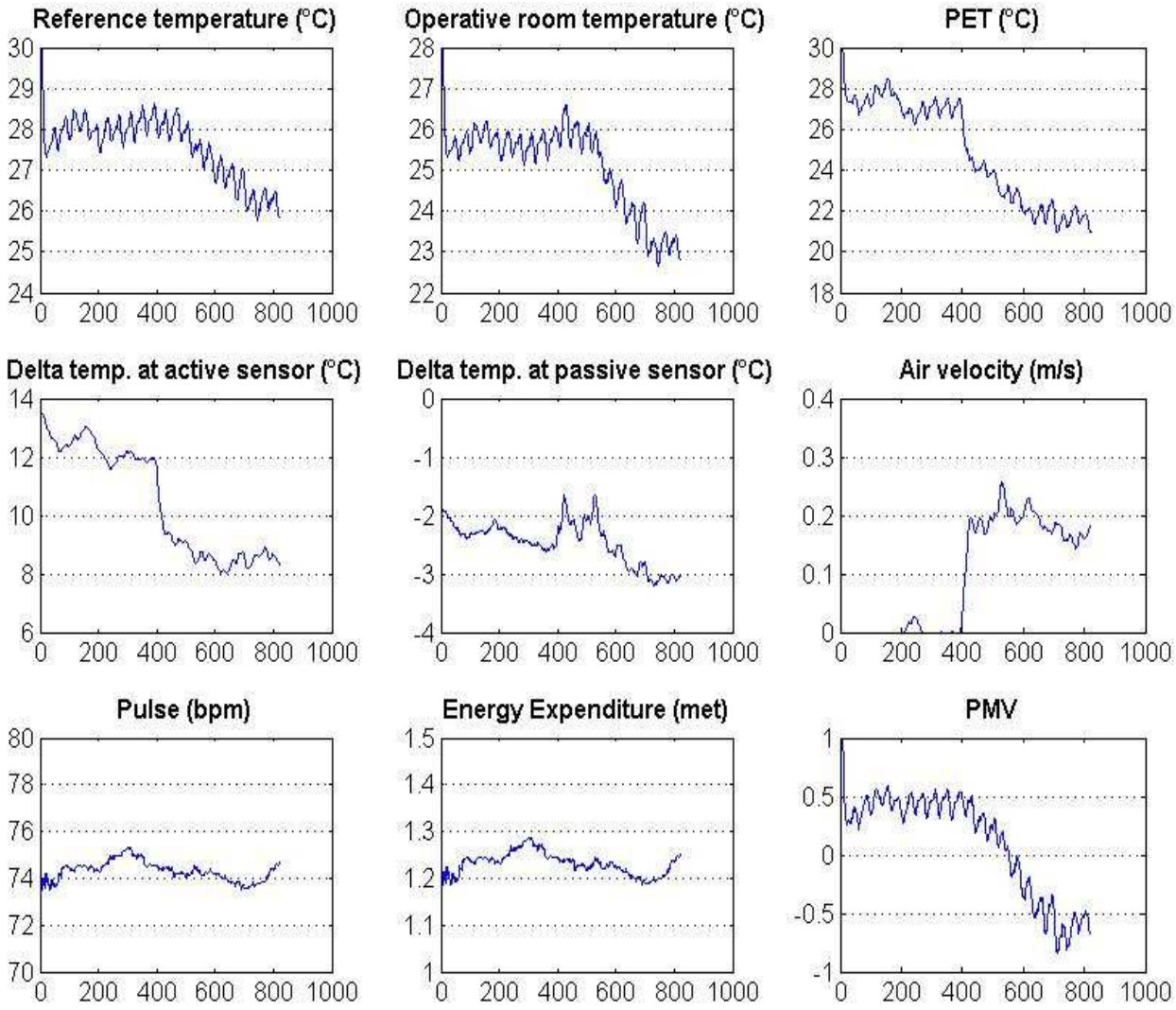

Figure 38: Measurement at point P4, Cooling mode

Measurement was begun with the air-conditioner off and operative room temperature of 26C. After 385 seconds the air-conditioner was switched on to cooling mode. Delta temperature at active sensor decreased from 12°C to 8.5°C and delta temperature at passive sensor slightly decreased from -2.5°C to -3°C. Measured air temperature was 0.2 m/s. Perceived temperature after cooling decreased from 27°C to 21°C and PMV decreased from 0.5 (slightly warm) to -0.5 (slightly cool).

8 Conclusion and Future Prospects

In the present work, a mobile prototype for thermal comfort measurement consisting of hardware and software for individual measurement of thermal comfort has been designed and made. The system consists of temperature, air velocity, and activity sensors and MICAz nodes for wireless data transmission.

This system can be applied not only for individual measurement and control of thermal comfort in which each person wears the sensor during the day. Another possibility is using this system for thermal comfort certification of an air conditioned room. The examiner only needs to wear the sensor to simulate the activity in the room for couple of hours.

For localization, an RSSI-based measurement method is proposed. The measurement result showed that RSSI pairs have special characteristic which points to pre-selected positions in the room. Three or more receivers are needed to detect the positions.

In the future development, an additional feature of automatic registration of a person who enters or exits the air conditioned room should be supported by this system. This registration will avoid the controller to include PMV from persons which are not inside the room.

Reference List

[Fan72] P.O Fanger, Thermal Comfort, Analysis and Application in Environmental Engineering, 1972

[DIN1946] DIN 1946 Teil 2 (Raumlufttechnik) – Gesundheitstechnische Anforderungen, 1994

[VDI3787] VDI 3787 Part 2: Methods for the human biometeorological evaluation of climate and air quality for urban and regional planning at regional level. Part I: Climate

[ISO7730] EN ISO 7730: Ermittlung des PMV und des PPD und Beschreibung der Bedingungen für thermische Behaglichkeit

[Höp84] Peter Höppe, Energiebilanz des Menschen, Wiss. Mitt. Meteorol. Inst. Uni München,1984

[Höp99] Peter Höppe, The Physiological Equivalent Temperature – a universal index for the biometeorological assessment of the thermal environment, 1999

[Bak98] Bonnie Bakers, AN679 Temperature Sensing Technologies, Microchip Technology Inc., 1998

[Spr99] The Measurement, Instrumentation, and Sensors Handbook, CRC Press Springer 1999

[Hii99] Hiiloskorpi, Pasanen, Fogelholm, Laukkanen, Mänttaäri Natri, Factors affecting the relation between heart rate and energy expenditure during exercise, 1999

[Hii03] Hiiloskorpi, Pasanen, Fogelholm, Laukkanen, Mänttaäri, Use of heart rate to predict energy expenditure from low to high activity levels, 2003

[TinyOS] TinyOS Tutorial http://www.tinyos.net/tinyos-1.x/doc/tutorial/

[Gab04] Thomas Gabriel, Studienarbeit S157: Implementierung eines AdHoc-Netzwerkes auf MICA2 Basis, TU-Kaiserslautern, 2004

[Ter06] Localization in Wireless Sensor Networks, Mark Terwillinger, Western Michigan University, 2006

[Mat99] Matzarakis, Mayer, Iziomon, Applications of a universal thermal index: physiological equivalent temperature, 1999

[UNU84] The United Nations University, Methods for the Evaluation of the Impact of Food and Nutrition Programmes, 1984
http://www.unu.edu/unupress/food/unu08/cap_13.htm

List of symbols and units

M	metabolic rate,in W
W	mechanical power, in W
$Q*$	radiation budget in, W
Q_H	turbulent flux of sensible heat, in W
Q_L	turbulent flux of latent heat (diffusion of water vapor), in W
Q_{SW}	turbulent flux of latent heat (sweat evaporation), in W
Q_{RE}	respiratory heat flux (sensible and latent), in W
$\frac{H}{A_{Du}}$	internal heat production per unit body surface are (A_{Du} : DuBois area)
I_{cl}	thermal resistance of the clothing
t_a	air temperature
t_{mrt}	mean radiant temperature
p_a	pressure of water vapor in ambient air
v	relative air velocity
t_s	mean skin temperature
$\frac{E_{sw}}{A_{Du}}$	heat loss per unit body surface area by evaporation of sweat secretion.